



Review

Modern insights of nanotheranostics in the glioblastoma: An updated review

Roopkumar Sangubotla^a, Kumar Shiva Gubbiyappa^b, Rajakumari Devarapogu^c,
Jongsung Kim^{a,*}

^a Department of Chemical and Biological Engineering, Gachon University, 1342 Seongnam Daero, Seongnam-Si, Gyeonggi-Do 13120, Republic of Korea

^b GITAM School of Pharmacy, GITAM Deemed to be University, Rudraram, Patancheru, Sangareddy Dist, 502329, Telangana, India

^c Department of Zoology, Sri Venkateswara University, Tirupati, Andhra Pradesh 517502, India.



ARTICLE INFO

Keywords:

Glioblastoma
Nanotechnology
Liposomes
Exosomes
Blood-brain barrier
Theranostics

ABSTRACT

Glioblastoma multiforme (GBM) is a highly malignant subtype of glioma, originating from the glial cells that provide support to other neurons in the brain. GBM predominantly impacts the cerebral hemisphere of the brain, with minimal effects on the cerebellum, brain stem, or spinal cord. Individuals diagnosed with GBM commonly encounter a range of symptoms, starting from auditory abnormalities to seizures. Recently, cell membrane-camouflaged nanoparticles (CMCNPs) are evolving as promising theranostic agents that can carry specific biological moieties from their biological origin and effectively target GBM cells. Moreover, exosomes have gained widespread scientific attention as an effective drug delivery approach due to their excellent stability in the bloodstream, high biocompatibility, low immune response, and inherent targeting capabilities. Exosomes derived from specific cell types can transport endogenous signaling molecules that have therapeutic promise for GBM therapy. In this context, researchers are utilizing various techniques to isolate exosomes from liquid biomarkers from patients, such as serum and cerebrospinal fluid (CSF). Proper isolation of exosomes may induce the clinical diagnosis in GBM due to their commercial accessibility and real-time monitoring options. Since exosomes are unable to penetrate the blood-brain barrier (BBB), strategic theranostic methods are ideal. For this, understanding interactions between glioma-specific exosomes in the TME and biomarkers is necessary. The versatile characteristics of NPs and their capacity to cross the BBB enable them to be indispensable against GBM. In this review article, we discussed the recent theranostic applications of nanotechnology by comparing the limitations of existing nanotechnology-based approaches.

1. Introduction

Based on their degree of malignancy, gliomas fall into four grades (WHO I, II, III, and IV), with type IV glioma, also known as glioblastoma (GBM), being the most fatal. Patients' survival rate and percentage curability are very low [1]. Although the etiology of GBM remains uncertain, it may be associated with ionizing radiation, smoking, dietary risk, or head injuries. GBM mostly affects the cerebral hemisphere, with a few cerebellar, brain stem, and spinal cord tumors. GBM patients include hearing and visual problems, increased intracranial pressure, and convulsions in 40 % of cases [2]. According to the 2020 CBRUS Statistical Report, the prevalence of GBM is increasing annually, with an incidence rate of 3.22 per 100,000 cases and a 5-year survival rate of 7.2 % [3,4]. GBM is associated with numerous genes, including those on

chromosomes 7 and 10, tensin homolog tumor suppressor genes, cyclin-dependent kinase inhibitors 2A and B, and the promoters of telomerase reverse transcriptase (TERT). In 70 % to 80 % of early GBMs, TERT promoter mutations decide how long the telomeric DNA is. These mutations are necessary for GBMs to become immortal and grow. About 40 % of initial GBMs had EGFR gene amplification, which increased tumorigenicity, cell proliferation, and apoptosis resistance. Secondary GBM spread more quickly when there were IDH1/2 mutations, more P53 proteins in the tumor, and X-linked thalassemia or mental retardation. Mutations in IDH1/2 are crucial for distinguishing secondary GBM from main GBM. Whether tumor-targeted treatment can correct IDH1/2 mutations is uncertain [5]. Secondary glioblastomas are thought to develop from a lower-grade glioma that advances or changes. Primary GBM has no recognized clinical antecedent [6,7]. The 2016 and

* Corresponding author.

E-mail address: jongkim@gachon.ac.kr (J. Kim).

<https://doi.org/10.1016/j.bbadis.2024.167653>

Received 29 August 2024; Received in revised form 8 December 2024; Accepted 28 December 2024

Available online 3 January 2025

0925-4439/© 2025 Elsevier B.V. All rights are reserved, including those for text and data mining, AI training, and similar technologies.

2021 WHO classifications and guidelines form the third category [8,9]. 70–80 % of low-grade gliomas, 5–10 % of main GBM, and secondary GBM show IDH1 and IDH2 mutations. This allows us to further subcategorize GBM into three groups: IDH-wild type (giant cell, gliosarcoma, epithelioid), IDH-mutant, and not otherwise described. Numerous standard approaches diagnose GBM. MRS, fMRI, and biopsy are therapeutically essential (Fig. 1). Palliative care usually becomes necessary after diagnosis due to limited options and poor quality of life. Since peptide-based delivery techniques may have off-target effects, we require a new early detection and noninvasive treatment strategy.

Over the past decade, “all-in-one” theranostic nanoplatforms that integrate diagnosis and therapeutics have improved brain cancer care. These include MRI/CT imaging before surgery, radiation therapy (RT), and chemotherapy after surgery. Their key benefits include sensitive early-stage tumor identification, real-time surgical planning and intra-operative surgery guidance, nanomedicine administration, PK/PD monitoring, and therapeutic treatment feedback monitoring. Photothermal and photodynamic therapies (PTT and PDT) are possible with several NIR nanoprobes. Laser irradiation induces nanoprobes to FLI or PAI, causing PTT hyperthermia or PDT ROS. Even though it is minimally invasive, very effective, simple to use, and has led to amazing advances, single-mode PTT or PDT cannot cure cancers because they are complex, varied, and heterogeneous [10]. Using photosensitive NPs along with non-invasive NIR irradiation is a more comprehensive way to treat diseases than traditional methods. The therapy platform achieves a high level of spatial and temporal treatment accuracy for aggressive and deeply seated GBM tumors, and this, in turn, makes NIR-based therapies safer. It's important to note that RGD-K peptides can specifically target $\alpha\beta3$ integrin receptors, and ALTS1C1 GBM cancer cells overexpress these receptors. For these reasons, researchers designed EuB6@RGD-K NPs through the surface modification of europium hexaboride (EuB6) NPs with the RGD-K peptide, which facilitated the strong adherence with these GBM cancer cells. EuB6@RGD-K NPs significantly target GBM cells by exerting their potential nanotheranostic effects under NIR-II (1064 nm) and NIR-III (1550 nm) light irradiations. EuB6@RGD-K NPs deliver exceptional photostability and a photothermal conversion efficiency (η) of 39.2 % under NIR-III (1550 nm) light irradiation. In addition, EuB6@RGD-K NPs can form abundant singlet O_2 through NIR-II 1064 nm photoexcitation and further generate excess hydroxyl radicals through NIR-III 1550 nm light irradiation. These EuB6@RGD-K NPs can facilitate combined PDT and PTT effects at NIR-II (1064 nm) and

NIR-III (1550 nm) wavelengths to destroy cancer cells in both in vitro and in vivo models [11].

Bangham et al. produced liposomes, vesicles containing an aqueous core and concentric phospholipid bilayers, in 1965 [12]. Liposomes have become popular for improving tumor-site specificity, therapeutic effectiveness, and encapsulating medication toxicity. The key reasons include biocompatibility, longer plasma circulation duration, prolonged biological half-life, biodegradability, and low immunogenicity. GBM treatment is intriguing for its use of lipid carriers as theranostic agents in gene delivery methods [13–16] Akbarzadeh and colleagues categorized liposomes as MLV, LUV, and SUV [17]. Unfortunately, traditional liposomes are unstable, short-lived, and rapidly release drugs into the bloodstream. Conventional methods for synthesizing liposomes include hydrating the lipid film using a French pressure cell, membrane extrusion, solvent injection, reverse phase evaporation, freeze-thaw extrusion, micro-emulsification, and removing detergents such as alkyl glycoside, Triton X-100, or cholate from mixed micelles [18–22]. In this regard, active ligand-functionalized liposomes and lipid nanocapsules (LNCs) have recently gained scientific interest for the GBM theranostic applications.

Due to their excellent blood circulation stability, biocompatibility, low immunogenicity, and natural targeting, exosomes are acting as promising nanotheranostic agents. Exosomes transport specific therapeutic components, such as proteins, nucleic acids, and lipids, to their surfaces, facilitating cell communication [23]. Exosome payloads vary by origin and biological state, which are crucial to GBM treatment. Receptor-ligand interactions deliver antigens, allowing exosomes to enter certain cells and fuse membranes to move surface proteins [24–26]. Exosomes' molecular makeup is identical to their CM, which prevents the immune system from picking them up, causing inflammation, or clearing them quickly [27–29]. Previous isolation procedures were tedious, non-commercial, and required extensive tuning, which slowed clinical diagnosis. Researchers can build simple and strategic glioma theranostic techniques by separating exosomes directly from patient blood and CSF for liquid biomarker investigations. We must examine new nanotheranostic-based glioma-specific exosomes.

Recently, nanomaterials have increased BBB permeability for GBM-targeted treatment. Combining therapeutic and diagnostic chemicals in a nanomaterial might provide dual GBM theranostics. The researchers created BBB-transportable NPs smaller than 14 nm for GBM theranostics. Researchers use poly(acrylic acid) to stabilize and alter

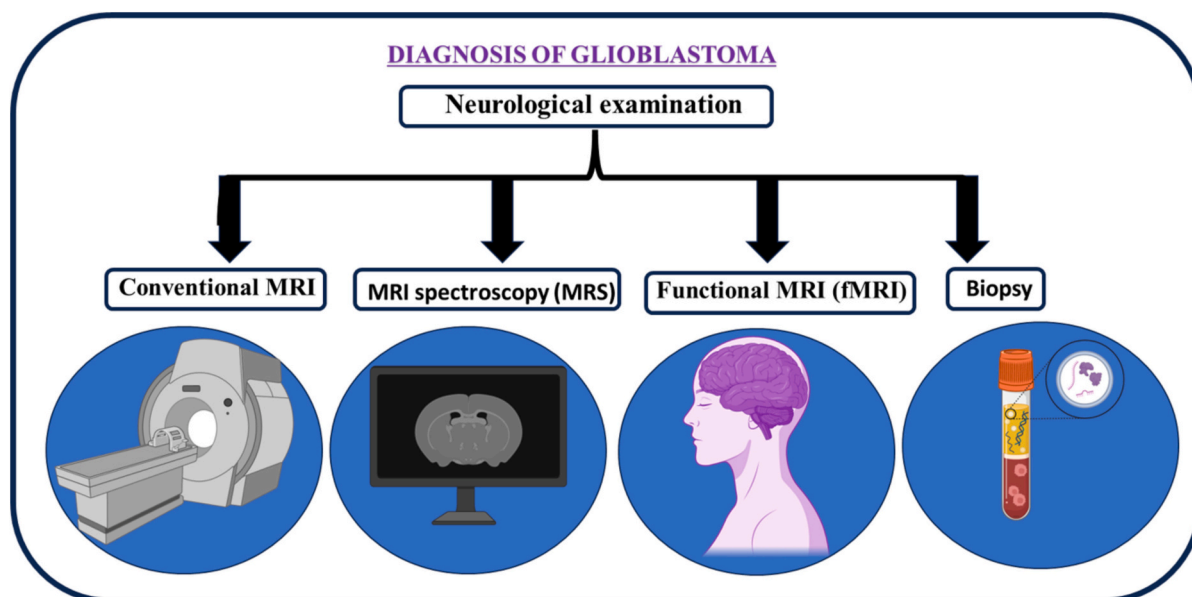


Fig. 1. Conventional neurological examination tests for the diagnosis of GBM.

extremely tiny gadolinium oxide NPs using reductive bovine serum albumin. The nanocomplex was biocompatible and could cross the in vitro and mouse BBBs due to its small particle size and structural tailorability. Researchers found ES-GON-rBSA3-LFRGD2 in orthotopic GBM, which means it might be useful as a radiosensitizing agent for treating GBM [30].

For the last decade, researchers have used zero-dimensional nanomaterials like graphene and carbon quantum dots (GQDs and CQDs) in GBM treatment due to their intriguing features. Researchers are exploring strategies to combat GBM that incorporate photophysical, ultra-nanoscale, electrochemical, fluorescence-tunable, and receptor-based targeting properties in PDT, PTT, and selective nanotheranostics. Transferrin-conjugated CQDs can traverse the BBB concentration- and time-dependently. Changes to their surfaces enable CQDs to use glucose transporters and passive diffusion to transport anticancer drugs from the blood to the brain [31].

In recent times, cell membrane-camouflaged nanoparticles (CMCNPs) are becoming more popular among researchers in clinical and theranostic applications because they are superiorly biocompatible and stay in the bloodstream for a long time [32]. Researchers employed cancerous cells, RBC, platelets, and macrophages to prepare hybrid membranes. The fact that CMCNPs can encapsulate biologically produced CMs and deliver specific medications to specific locations reduces off-target accumulation. Therefore, reducing side effects can enhance therapeutic effectiveness against GBM, particularly when CMCNPs carry specific theranostic agents. This review focuses on the recent advancements in various nanomaterials used in nanotheranostics applications for treating GBM. We also discussed various approaches, existing limitations to nanomaterials, and explored future directions in GBM therapy.

2. Convection enhanced delivery of nanocarriers in GBM therapy

Bobo et al. introduced CED in 1994 [33]. CED may provide a variety of benefits. In contrast to diffusion-limited delivery, CED improves interstitial medication dispersion with pressure. Localized administration reduces neurotoxicity because infused dosages are lower than diffusion-mediated distribution. Compared to implanted polymers, CED may not increase brain damage risk [34]. The CED method in animals and humans has found transitory and reversible neurological effects in the eloquent regions with lower infusion rates [35,36]. Even molecules as small as 80 kDa at first have a linear relationship with the volume of distribution (Vd) of the infusate. The strong backflow around the infusion catheter at specific speeds is responsible for this phenomenon [33]. CED device improvements should reduce backflow and improve Vd-Vi relationships, enabling higher infusion rates. The tissue cytoarchitecture can influence the variation in Vd from the CED [37,38]. The CED of a GBM has few blood vessels and a mixed cytoarchitecture, which means it contains a large number of blood vessels but also some that are not functioning properly. A leaky cytoarchitecture and an outward pressure gradient contribute to an increase in infusate clearance. Regional anisotropy and white matter edema may also promote infusion. CED may also reach tumor cells at the margin and disseminate them more uniformly without a craniotomy or steroids, according to a new study [39]. Tissue properties and catheter-caused backflow likely slowed down early clinical trials. However, researchers have made this method better by altering the conditions of the infusate and cannula, creating guidelines for where to place the catheter, using algorithms to predict its location, and observing the infusate delivery in real-time. Researchers deliver CED chemotherapy to GBM tumors and surrounding tumor-infiltrated brains [40–42]. The CED technique conducted clinical trials to explore the benefits of topotecan, demonstrating a 23-week progression-free survival and a 60-week overall survival [43,44]. The investigation followed the injection of topotecan into the brainstems of two young patients with diffuse intrinsic pontine gliomas in 2013. In this regard, it is suggested that lowering infusion rates and drug

concentrations is better due to the vulnerability of the brainstem to local chemotherapy than other brain regions and increased fluid infusion side effects [35]. Fiandaca and colleagues initially hailed a step-design cannula as a breakthrough in CED catheter technology. They created this cannula with a 0.2 mm needle and glued-in silica tubing (0.168 mm external diameter), extending 5–10 mm beyond the needle [45]. The PRECISE experiment indicated large changes and proved that catheter implantation was beneficial. Researchers developed software algorithms to determine the optimal intraoperative navigation system courses for neurosurgeons [46]. Numerous previous studies have also discovered that the CED technique's brief catheter implantation can only last a limited time. Consequently, researchers are currently developing a solution for humans after testing it on primate models. Table 1 summarizes completed and ongoing clinical trials for GBM therapy using CED technique.

3. Nanotechnology-based approaches for GBM theranostics

Until the advent of nanotechnology, researchers and medical professionals relied on other contemporary approaches: (i) immunotherapy, (ii) genetic engineering, (iii) drug delivery, and (iv) nanomedicine, etc. (Fig. 2). Among these, nanotechnology-based therapy has gained popularity due to its versatility, biocompatibility, cost-effectiveness, etc. Specifically, its non-invasiveness and enhanced surface-to-volume ratio properties make it engaging for its broad applicability in major clinical settings. Till now, a myriad of nanoscale materials has been available, which include liposomes, LNCs, exosome vesicles, NPs, etc. Under the following section, we discuss different forms of nanomaterials used in GBM therapy, with a special emphasis on detailed biological and drug-related characteristics. So far, numerous NPs are available for GBM therapy, which includes metal-based NPs, magnetic, silica, and polymeric NPs. Fig. 3 illustrates nanomaterial-based GBM management therapy. The ideal NPs for GBM therapy should have the following desirable properties: (i) excellent adaptability; (ii) controlled physicochemical attire (size, diameter, optical, electrical, and chemical properties); and (iii) a high surface/volume ratio.

3.1. Metal-based nanoparticles

Metal-based NPs have the potential to increase the sensitivity of GBM tumor cells to radiation. In animal models, treating tumor cells with metal particles prior to radiation therapy resulted in significant DNA damage [47]. High X-ray absorption, synthetic adaptability, and unique electrical properties are desired features for metal-based NPs, making them attractive candidates for radiosensitizers [48]. In the treatment of GBM, gold nanoparticles (AuNPs) stand out among noble metal inorganic NPs due to their size tunability and desirable surface/volume ratio. Due to their regulated size, AuNPs can easily cross the BBB, but their lack of targeting abilities limits their clinical applicability. Recently, researchers developed AuNPs-based DNA aptamers for targeting EGFRvIII in GBMs using a large random single-stranded DNA, where gold-sulfur covalent interactions effectively trap the aptamer, resulting in the effective targeting abilities. Liu et al. showed that aptamer-AuNP complexes are a new type of therapeutic candidate for GBM therapy, which significantly fight against GBM by reducing tumor growth [49]. Recently, researchers have employed gold-iron oxide NPs to deliver therapeutic gene targets, i.e., miR-100, a tumor suppressor. When given to mice, these gold-iron oxide NPs made GMB cells more sensitive to TMZ [50]. Previous studies have demonstrated that metal-based NPs are cytotoxic with undesired damage to normal tissues after long-term accumulation in circulation. Unfortunately, metal-based NPs are harmful due to several issues, including oxidative stress, the release of inflammatory cytokines, the breaking down of lysosomes, and DNA damage [51]. The USA Food and Drug Administration (USFDA) has already approved several gold and silver nanoformulations containing chemotherapeutic drugs for clinical studies due to their well-established

Table 1

List of completed and ongoing clinical trials for the treatment of GBM using CED.

S. no.	Title	Treatment	Phase	Clinical Trials.gov reference no:
1	Trial of Intraparenchymal-administered topotecan using convection-enhanced delivery (CED) in patients with suspected recurrent/progressive WHO Grade III or IV (high-grade) glioma requiring stereotactic biopsy	Drug: Topotecan, Gadolinium DTPA Device: Cleveland Multiport Catheter	Early phase 1	NCT02278510
2	Study of intratumorally and intraparenchymal-administered OS2966 Using CED in patients with recurrent/progressive high-grade glioma undergoing a clinically-indicated surgical resection	Drug: OS2966, Gadoteridol	Phase 1	NCT04608812
3	Chronic CED of topotecan for recurrent high-grade gliomas	Drug: Topotecan, Gadolinium Device: Synchromed II infusion pumps	Phase 1	NCT03154996
4	An open-label non-randomized, multi-center study of CED of MDNA55 in adults with recurrent or progressive glioblastoma	Drug: MDNA55	Phase 2	NCT02858895
5	An open label single arm study of MTX110 Delivered by CED in patients with diffuse intrinsic pontine glioma (DIPG) previously treated with external beam radiation therapy	Drug: Panobinostat Nanoparticle Formulation MTX110	Phase 1 & 2	NCT03566199
6	Study of CED of 124I-Omburtamab for patients with non-progressive diffuse pontine gliomas previously treated with external beam radiation therapy	Drug: Radioactive iodine-labeled monoclonal antibody omburtamab Radiation: external beam RT	Phase 1	NCT01502917
7	Study Examining the Feasibility of Intermittent CED of MTX110 for the treatment of children with newly diagnosed diffuse midline Gliomas	Drug: Infusate with MTX110 and gadolinium	Phase 1	NCT04264143
8	Study of CED of IL13-PE38QQR infusion after resection followed by radiation therapy with or without TMZ in patients with newly diagnosed supratentorial malignant glioma	Drug: IL13-PE38QQR Procedure: surgery for placement Procedure: radiation therapy Drug: TMZ with RT	Phase 1	NCT00089427
9	Randomized Evaluation of CED of IL13-PE38QQR compared to GLIADEL® Wafer with	Drug: IL13-PE38QQR Procedure: surgery and catheter placement (2	Phase 3	NCT00076986

Table 1 (continued)

S. no.	Title	Treatment	Phase	Clinical Trials.gov reference no:
	survival endpoint in GBM patients at first recurrence	procedures) Drug: prolife span 20 with carmustine implant (GLIADEL® Wafer) Procedure: surgery and wafer placement (1 procedure)		
10	Intracerebral CED of Carboplatin for treatment of recurrent high-grade gliomas	Drug: carboplatin Procedure: Surgery	Phase 1	NCT01644955
11	Trial of D2C7-IT in combination with an Fc-engineered Anti-CD40 monoclonal antibody (2141-V11) administered intratumorally via CED for adult patients with recurrent malignant glioma	Drug: D2C7-IT Drug: 2141-V11	Phase 1	NCT04547777
12	Dose escalation study of D2C7-IT administered intratumorally via CED for adult patients with recurrent malignant glioma	Drug: D2C7-IT	Phase 1	NCT02303678
13	Early efficacy study of CED of Irinotecan liposome injection using real-time imaging with gadolinium in children with diffuse intrinsic pontine glioma	Drug: CED of nanoliposomal irinotecan (nal-IRI)	Phase 1	NCT03086616
14	Conditionally replication-competent adenovirus (Delta-24-rgd) administered by CED for patients with recurrent glioma	Biological: delta-24-RGD adenovirus	Phase 1 & 2	NCT01582516
15	Interstitial infusion of IL13-PE38QQR cytotoxin in recurrent malignant glioma	Drug: IL13-PE38QQR Procedure: targeted fusion protein therapy Procedure: surgery	Phase 1 & 2	NCT00024570
16	Study to assess the histologic effect and safety of pre-operative and post-operative infusions of IL13-PE38QQR cytotoxin in patients with recurrent resectable supratentorial malignant glioma	Drug: IL13-PE38QQR Procedure: targeted fusion protein therapy Procedure: surgery	Phase 1	NCT00024557
17	Multi-national, open-label, active-controlled, randomized dose-finding study to evaluate efficacy of 2 doses of AP 12009 in recurrent glioma, administered intratumorally as continuous high-flow micro-perfusion over 7 days every other week	Drug: AP 12009 10 µM Drug: AP 12009 80 µM Drug: TMZ or PCV Device: Drug delivery system for administration of AP 12009 Procedure: Placement of drug delivery system	Phase 2	NCT00431561

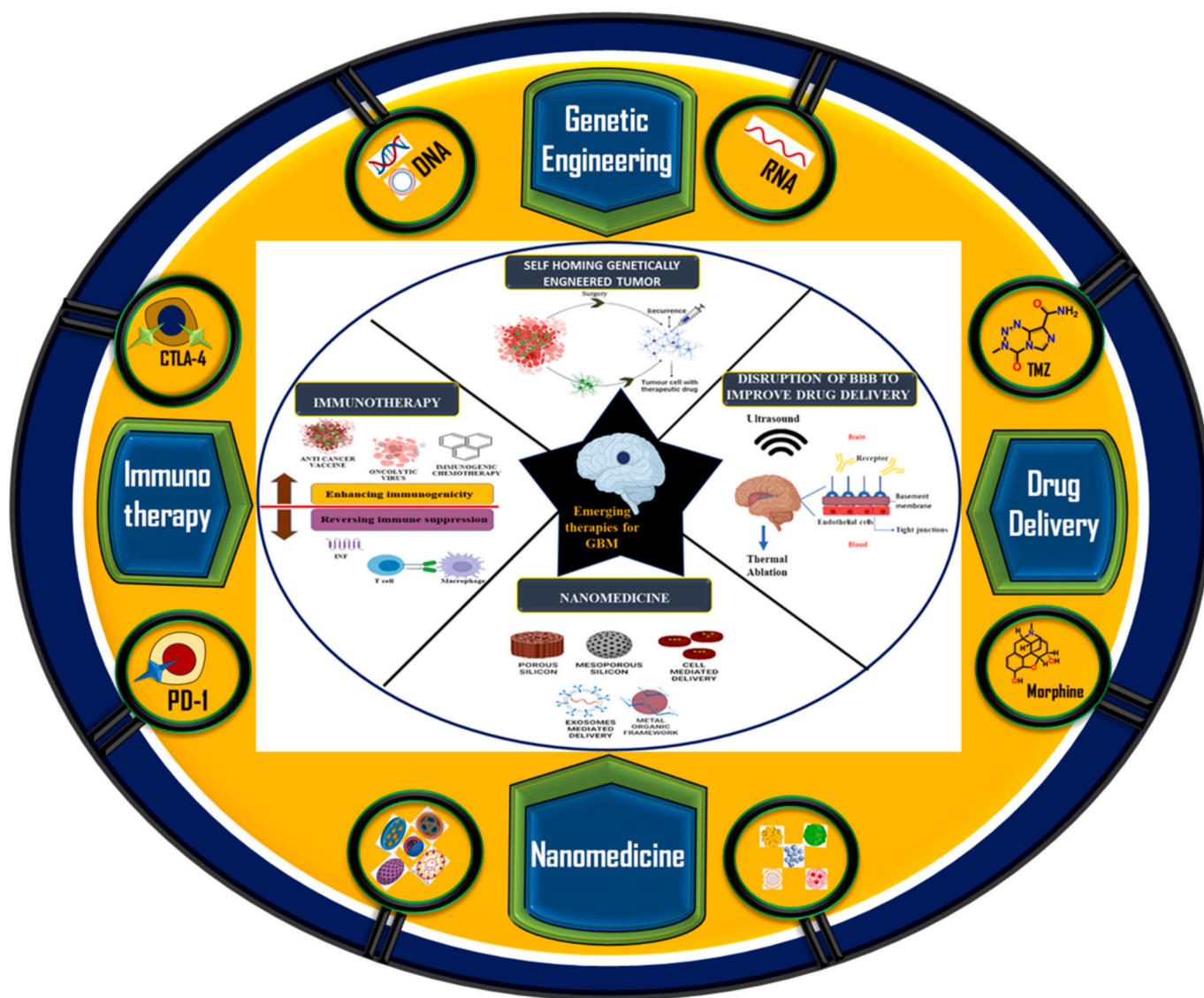


Fig. 2. Emerging therapies for the GBM including immunotherapy, genetic engineering, drug delivery, and nanomedicine.

biodistribution and clearance rates [52].

Luque et al. developed polymeric NPs (PNPs) containing superparamagnetic iron oxide NPs (SPIONs) and DOX for tailored therapy. Both approaches have therapeutic potential, but the former concentrates PNPs in magnetically stimulated tumors. The emulsion solvent and evaporation method produced dispersed PNPs with high SPION and DOX loading efficiencies. In injected rats, MRI showed that PNPs accumulated in tumoral tissue under a static magnetic field, inhibiting tumor development [53]. The authors made a nanobubble (NB) from a chemotherapy medication and additional nanomaterials to track and route the nanocomposite to the tumor. The authors loaded iron-platinum (FePt) NPs and DOX into NBs with hydrophobic cores to design a bubble-based drug delivery system. High-intensity focused ultrasonic oscillation ruptures the NBs, briefly cavitating the BBB and allowing drug to enter the brain. Targeting ligand transferrin (Dox-FePt@NB-Tf) to the NBs' surfaces enhances the nanocomposite's active tracking characteristics. Dox-FePt@NB-Tf has the potential to transform GBM treatment through enhanced drug delivery and biological monitoring [54]. A multifunctional agent with strong BBB penetration is ideal for accurate theranostics. Researchers developed effective core-shell nanotheranostic agents (YHM) for GBM therapy, incorporating yttrium vanadate (YVO₄) and neodymium (Nd) NPs (YVO₄:Nd³⁺) as the core and

MnO₂ nanosheets as the shell. Additionally, the sonosensitizers lactoferrin (LF) and hematoporphyrinmonomethyl ether (HMME) were incorporated into NIR-II/MRI bimodality-based YHM, enabling them to cross the BBB and assist in the treatment of orthotopic gliomas using sonodynamic therapy (SDT). The YVO₄:Nd³⁺ core had strong NIR-II fluorescence, which made YHM a useful probe for imaging blood vessels and gliomas that are not in the right place. The MnO₂ shell gives off Mn²⁺ ions, which makes in situ T₁-weight MRI easier. It also speeds up the SDT process by bringing oxygen to the TME [55]. The multifunctional agents mentioned above, possessing strong BBB penetration, are highly suitable as nanotheranostics for GBM therapy.

Most biomedical applications use magnetic NPs (MNPs) due to their biocompatibility. In comparison to conventional contrast agents, SPIONs have exceptional optical and magnetic susceptibility, making them a suitable choice for MRI. Also, changes in SPIONs' surface and chemical makeup made it easier to find malignant tumors [56]. Future treatments for GBM could potentially include therapeutic hyperthermia (MHT). Researchers have discovered that SPIONs can consistently enter the intertumoral space and control how hot the GBM gets without having any major side effects [57–59]. Researchers have also used hyperthermia as a new mechanism to increase drug delivery to tumors. It has several advantages, including ease of manufacture, excellent

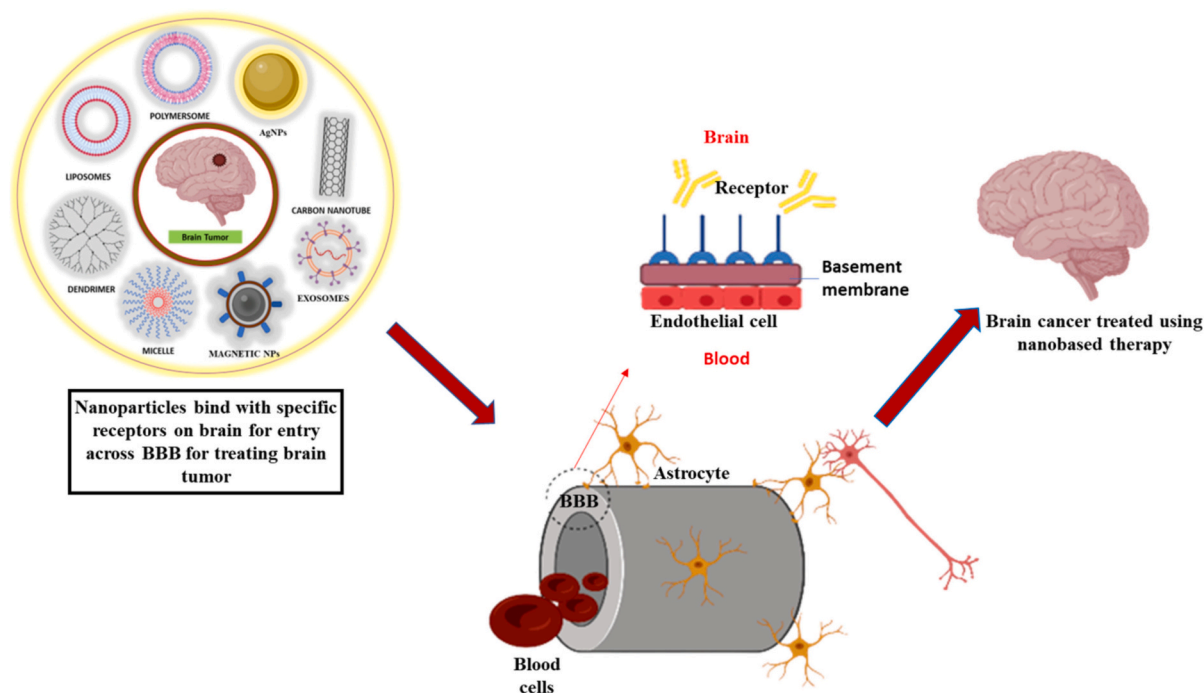


Fig. 3. Schematic illustration for the nano-based therapy in the brain cancer.

biocompatibility, and low cost. SPION-based hyperthermia has several advantages, including the ability to cross the BBB, multiple delivery routes, minimal or no side effects, and the fact that it is technically non-invasive [60,61]. The authors characterized gold nanorods (GNRs) using their optical properties, which vary depending on their size. The most significant feature of GNRs is surface plasmon resonance (SPR). This phenomenon occurs when gold atom electrons in a transmission band interact with the electric field components of electromagnetic radioactivity [62]. Due to their unique physical and optical properties, GNRs can release heat when exposed to a near-infrared (NIR) laser via SPR, making them novel PTT agents for the GBM therapy. Many studies have leveraged this property to improve GBM PDT. Because of their high biocompatibility, GNRs have sparked a lot of interest in hyperthermic therapy [63]. In vivo, injecting GNRs into a vein and exposing them to NIR laser light can kill GBM cells by heating and killing them. Several studies have shown that attaching PEGylated GNRs to an Arg-Gly-Asp sequence can effectively target AVb3 integrins found on GBM cells for anti-tumor therapy using high temperatures. All studies have employed folate-conjugated GNR to target cancer cells. Therefore, we can precisely target GBM cells using folate-conjugated GNRs [64,65]. Numerous studies have demonstrated that a NIR laser can excite folate-conjugated GNRs, potentially targeting and killing GBM cells. When NIR light hit PEGylated GNRs, they released DOX from thermosensitive liposomes, which was used as a model for human GBM [66]. Flow cytometric analysis revealed that GNRs attached to DOX and cyclo (Arg-Gly-Asp-D-Phe-Cys) peptides were more effective at killing and entering cells than GNRs that were not targeted and attached to DOX [67].

3.2. Non-metal-based theranostic approaches

3.2.1. Liposomes and lipid nanocapsules

Among many existing nanomaterials, liposomes were considered the first FDA-approved therapeutic drugs for cancer [68]. According to several previous studies, polyethylene glycol (PEG)-modified liposomes prolong their systemic circulation. Passive diffusion through various transcellular pathways is important for delivering drugs into glioma cells. These include cell-mediated transcytosis (CMT), transporter-mediated transcytosis (TMT), receptor-mediated transcytosis (RMT),

and adsorptive-mediated transcytosis (AMT). The AMT route enables peptides to enter cells and adhere to liposomes. Inside the cells, they interact with the negatively charged membrane of brain microvascular endothelial cells (BMECs). Endocytosis allows liposomes to enter glioma cells via the BBB/BBTB. RMT, which delivers drugs into the brain without surgery, is helpful in treating gliomas [69]. Especially endogenous molecules like transferrin and insulin are capable of binding to BMEC receptors and traversing the BBB [70]. Until now, researchers have investigated multifarious receptors, including neonatal Fc, leptin, nicotinic acetylcholine, nucleolin, folate, insulin, and low-density lipoproteins, to deliver drugs to glioblastoma. After binding to its specific receptor on the inner side of the endothelial cell, the complex moves into the cytoplasm and then moves out to the brain parenchyma [71–73]. CMT allows leukocytes and stem cells to transport drug-loaded liposomes across the BBB [74,75].

As natural inflammatory cells, leukocytes may penetrate the BBB to deliver drugs to inflamed brain regions and form extracellular traps to release the pharmaceuticals. Leukocytes such as neutrophils (NEs), monocytes, and macrophages modify liposomes to penetrate the brain and treat GBM. In one study, researchers extracted an attenuated bacterial membrane (BM) from *Salmonella typhimurium* VNP20009 and conjugated it with phospholipids to construct liposomes [76]. B-Lipo/1-MT&Cur NPs were synthesized by functionalizing with hydrophilic and hydrophobic drugs, including 1-methyl-D-tryptophan (1-MT) and curcumin (Cur), respectively (Fig. 4, I). Researchers studied the morphological features of B-Lipo/1-MT&Cur through TEM analysis, revealing a liposome-like structure with an average size of 100 nm (Fig. 4, II). For this purpose, researchers purified mouse bone marrow NEs by density gradient centrifugation (DG) using percoll solution and obtained liposome-carried NEs by incubating B-Lipo/1-MT&Cur and Lipo/1-MT&Cur with NEs for 6 h. Mixing these suspension cells with adherent mouse glioblastoma cells (GL261) allowed the GL261 cells to absorb the drugs released by the NEs (Fig. 4, III). NEs absorbed B-Lipo/1-MT&Cur more effectively than Lipo/1-MT&Cur, thanks to the enhanced adherence of liposomes to the cells, supported by the surrounding BM (Fig. 4, IV). During inflammation, NEs release significant amounts of Cur, which the tumor cells absorb. This shows that the NEs can release their drugs for GBM therapy (Fig. 4, V). The amount of B-Lipo/1-MT&Cur in the

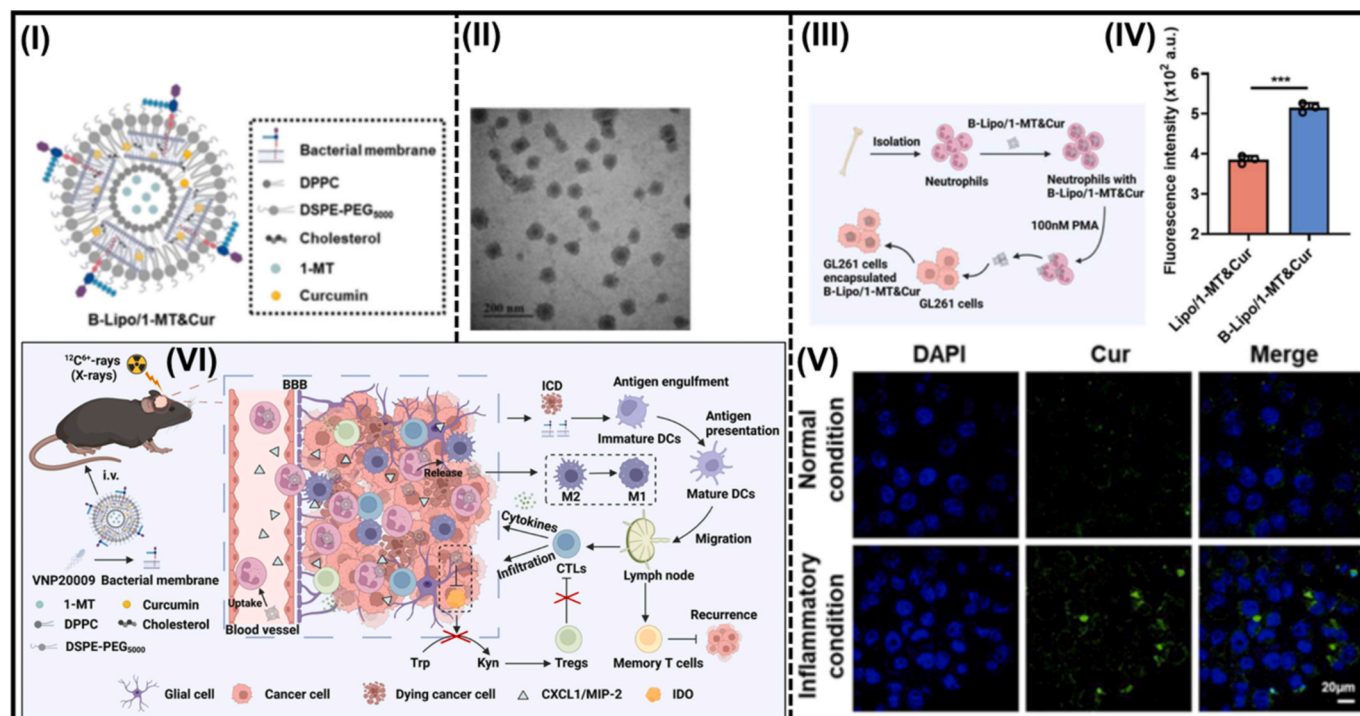


Fig. 4. Synthesis and characterization of B-Lipo/1-MT&Cur. (I) Structure diagram of B-Lipo/1-MT&Cur, (II) TEM image of B-Lipo/1-MT&Cur, (III) Schematic representation of the uptake and release of B-Lipo/1-MT&Cur by neutrophils. (IV) Flow cytometry analysis of neutrophils incubated with B-Lipo/1-MT&Cur or Lipo/1-MT&Cur for 6 h ($n = 3$). (V) Confocal images of GL261 cells incubated with B-Lipo/1-MT&Cur-loaded neutrophils under normal and inflammatory condition (PMA, 100nM). (VI) The schematic diagram showing the radiotherapy-mediated B-Lipo/1-MT&Cur targeting to glioblastoma and the synergistic carbon ion/X-rays radiotherapy and chemo-immunotherapy of existing glioblastoma and its recurrence. Reproduced with permission from Nanotoday, [76]. Copyright 2023, Elsevier Ltd.

tumor went up after RT, which increased the ratio of ICD and CTL/Treg tumor cells. B-Lipo/1-MT&Cur altered the immunosuppression by shifting macrophages from M1 to M2 and increasing IDO expression. These changes made the immune system stronger against tumors. Using $^{12}\text{C}^{6+}$ -rays, the combined treatment may cure most orthotopic GL261-bearing mice, and anti-tumor immunological memory also halted the growth of GL261 cells upon rechallenge. This suggested that the above-mentioned method mitigated the recurrence of GBM. Therefore, the clinical use of carbon ion RT-assisted immunotherapy may offer hope to cancer patients (Fig. 4, VI).

Kuang and his colleagues designed endogenous cell hitchhiking NPs to cross the BBB for tailored drug delivery [77]. NPs (D@MLL) carry doxorubicin (DOX) to brain GBM sites where it can be released precisely by low-dose local RT. D@ML is a peptide-liposome that responds to MMP-2 and encapsulates DOX. Lipoteichoic acid (LTA) changed the surface of D@ML by connecting to monocytes through the CD14 receptor (Fig. 5A). Starting with low-dose RT at the tumor site, we changed the shape of tumor-associated monocytes (TAMs) M1 and increased the expression of CCL-2 (Fig. 5B). After IV injection, D@MLL hitchhiked with monocytes to the central GBM area. High tumor MMP-2 concentrations cleaved the PLGVR peptide between G and V amino acids. Breaking the peptide-liposome structure released DOX. This killed the GBM cells through immunogenic cell death (ICD). Tumor cells released calreticulin (CALR) and high-mobility group box 1 (HMGB1). Fig. 5C demonstrated that these proteins enhanced the activity of TAM M1-type cells, DC maturation, and CD8-positive T cells.

For the first time, researchers studied macrophage membrane liposomes (MML) from normally activated macrophages (M1) and alternatively activated macrophages (M2) as a way to deliver drugs to GBM cells [78]. Researchers also investigated the polarization states of macrophages and the characteristics of their membranes in relation to DDS. Researchers synthesized MML by polarizing macrophages, separating

their membranes, and fusing nanocarriers together (Fig. 6, I, and II). Researchers also investigated the expression of membrane proteins, which could potentially explain the changes in Dox absorption and delivery among GBM cells with M1 and M2 MML. The axis of VCAM-1/CD49d, membrane proteins produced by cancer and myeloid cells, establishes a connection between macrophages and cancer cells. Further, we examined the expression of VCAM-1 in U87 GBM cells using immunofluorescence (Fig. 6, IIIa). Researchers examined the expression of CD49d in macrophages at different stages of polarization (Fig. 6, IIIb). M1 macrophages expressed less CD49d than M0 and M2 (Fig. 6, IIIc).

Researchers have also investigated micro-RNAs, non-coding RNAs, as potential novel therapeutics. Several GBM samples have lower amounts of miR-181a-5p, and this gene's overexpression stops tumor growth in both vitro and vivo. The authors synthesized a modified lipid-based nanocarrier that could encapsulate and deliver miR-181a to GBM cells. The authors also incorporated layers of poly-L-arginine and hyaluronic acid (HA) onto the lipid nanoparticles (LNPs) containing miR-181a. The hyaluronan-coated HA-LNPs effectively delivered siRNA and miRNA, and they were better at targeting GBM cells than unmodified LNPs. Finally, HA-LNPs delivered miR-181a, which can kill U87 GBM cells and slow the growth of skin tumor models, which is a good result [79]. Other studies demonstrate that the ApoE-modified SLNs could pass through a BBB model without structural damage. Their investigation also showed that ApoE-modified SLNs internalized more cells than non-functionalized ones. Glioma, vasculogenic mimicry (VM), and BBB cells all overexpress the 78-kDa glucose-regulated protein GRP78. It binds well to the D-peptide ligand VAP. At the same time, p-hydroxybenzoic acid (pHA) can cross the BBB. Wu et al. synthesized cabazitaxel (CBZ) nanocrystal-encased liposomes containing VAP and pHA composite ligands [80]. In vitro studies demonstrated that pV-Lip/cnC targeted gliomas, crossed barriers, and penetrated the tumor spheroid. Adding more CBZ to gliomas with PV-Lip/cnC improved the

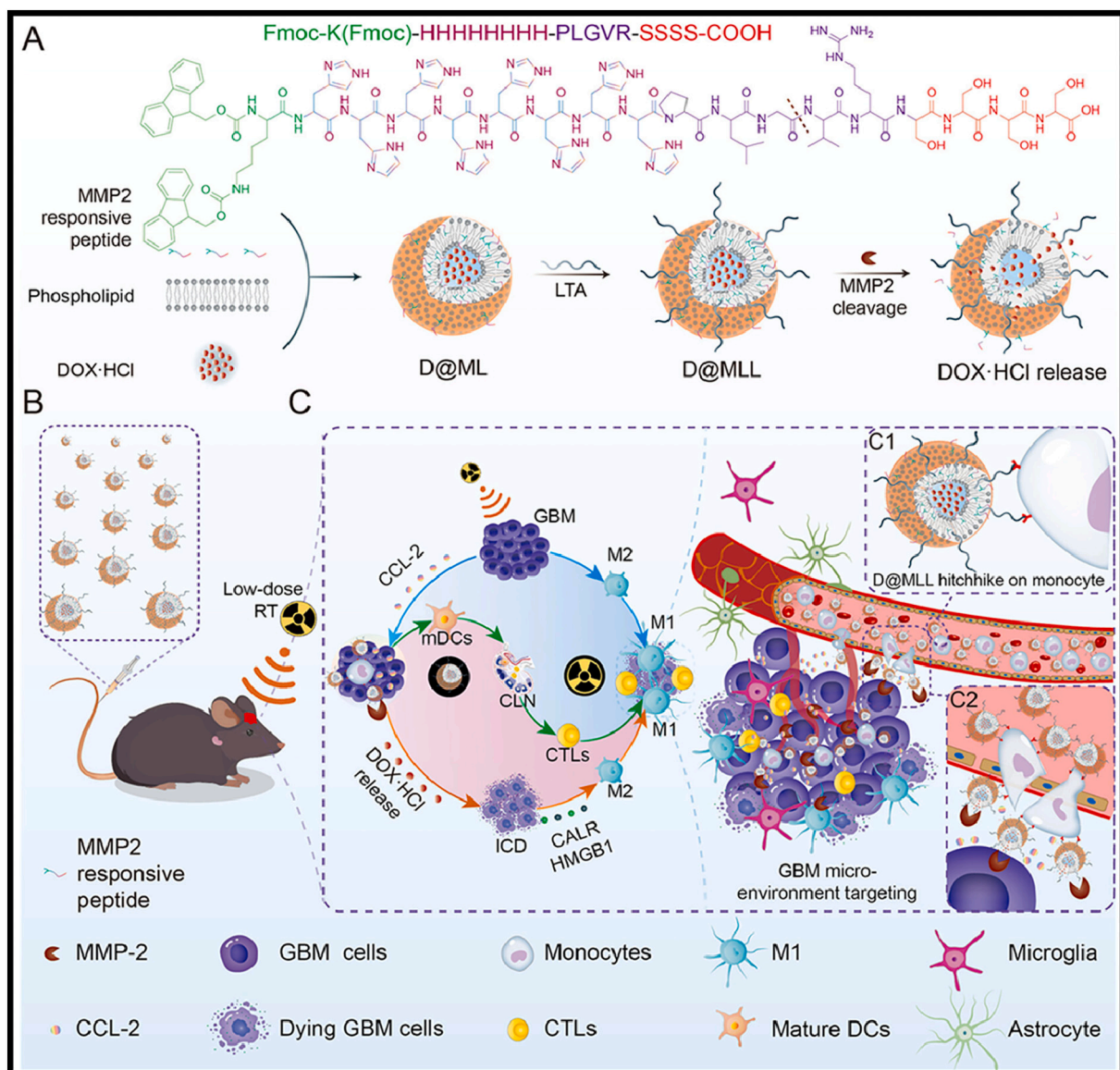


Fig. 5. Schematic of D@MLL hitchhike on monocytes for GBM treatment after low-dose RT. (A) synthesis of D@MLL. (B) D@MLL intravenously injected to GBM bearing mice after low-dose RT. (C) anti-GBM effects induced by D@MLL with low-dose RT. (C1) D@MLL hitchhike on circulating monocytes, (C2) crossing the BBB with the assistance of CCL-2 and Releasing DOX-HCl via MMP-2 response. Reproduced with permission from ACS Nano, [77]. Copyright 2023, ACS publications.

effectiveness of anti-glioma drugs. The average survival time in a mouse model of orthotopic GBM increased to 53 days. Based on these results, pV-Lip/cNC may be able to cross the BBB and BBTB and kill glioma cells, which makes it a potentially useful treatment for GBM [81]. Table 2. summarizes a list of some of the liposomes used in glioma management [82–88].

The LNCs are a hybrid structures between liposomes and polymeric NPs and consisting of a solid lipid and emulsifying agent shell surrounding an oily core. LNCs have been shown to be useful in treating glioblastoma because they are biodegradable, biocompatible, small (20 to 100 nm), stable, and encapsulate numerous lipophilic drugs [89–91]. Since the core of LNCs encloses the drug, it shields it from degradation and poses no harm to healthy cells [92]. Liquid lipids, usually oils, make up the core of LNCs, whereas solid lipids make up the shell [93]. The oily phase serves as a drug reservoir, accounting for 10–25 % of the LNCs by weight. Medium-chain triglycerides, such as capric acid and caprylic acid triglycerides, make up the oily phase and act as penetration enhancers [94,95]. Lecithin is primarily a lipophilic surfactant. It comes in two varieties: lipid (a co-surfactant) and phospholipon. Phospholipon

is a combination of hydrogenated lecithin and phospholipids found in nature. In comparison to Solutol, lipid has reduced surface-active characteristics. Lipid-integrated LNCs have a smaller diameter. Lipid in higher concentrations in the formulation may better react with Solutol, which acts as a co-surfactant, stabilizing the formulation. After freeze-drying, we should compromise the solutol/lipoid ratio to preserve the stability and biopharmaceutical performance of LNCs [96]. The non-ionic surfactant makes up 10–40 % of the LNCs by weight. The chain length of PEG (polyethylene glycol) is believed to impact the temperature required for phase inversion [97]. Non-ionic polyethoxylated surfactants play a significant role in the phase inversion of emulsions. The most frequent type of solutol is PEG-derived solutol. It is amphiphilic because it contains both hydrophilic PEG and hydrophobic hydroxystearate [93,97]. As a result, it has significant surface-active characteristics and is impacted by the triglyceride/water interface. The percentage of Solutol is inversely proportional to the particle size of LNCs [97]. The mononuclear phagocyte system quickly detects and clears NPs injected into the bloodstream as foreign entities. Researchers have found that PEG and its derivatives can help with stearic repulsion

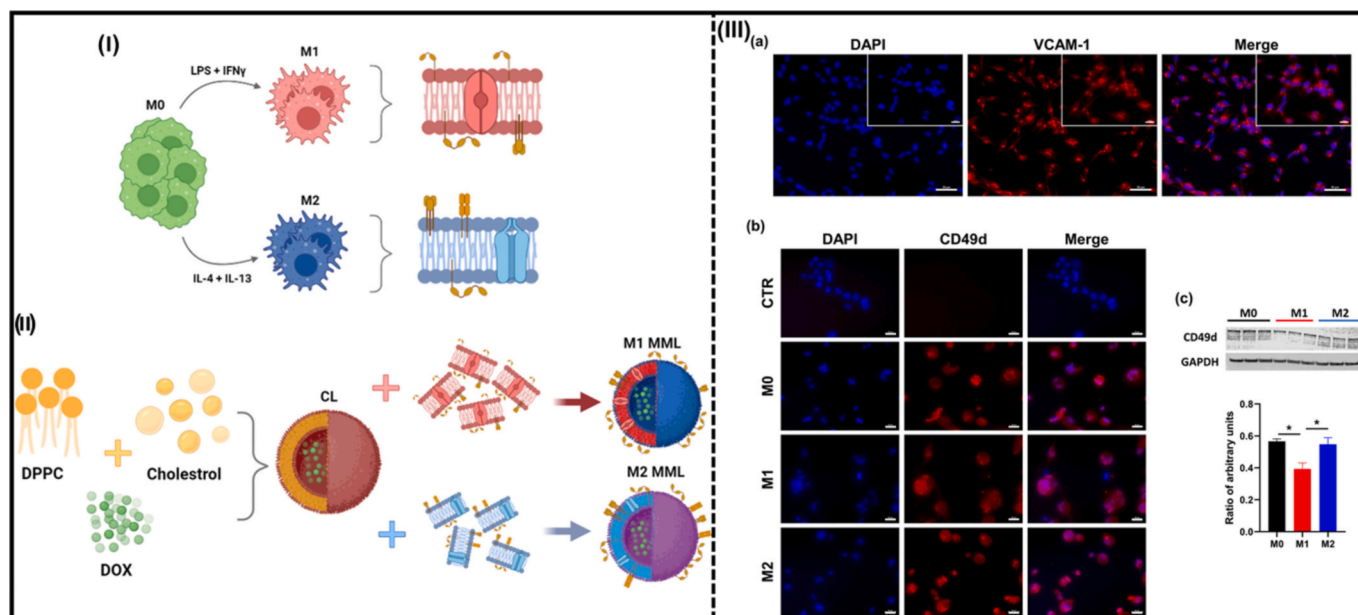


Fig. 6. Schematic illustration of macrophage membrane liposomes (MML) preparation. (I) Polarization of macrophages for a classically activated phenotype (M1) and alternatively activated phenotype (M2). (II) Composition and preparation of liposomes by fusion with macrophage membrane to create MML. (III) Role of VCAM-1/CD49d Axis in MML Delivery systems (a) VCAM-1 expression was confirmed in U87 cells by immunofluorescence. (b) Macrophages (M0, M1 and M2) expression of CD49d detected by immunofluorescence. (c) Western Blot analysis of CD49d and respective quantification in the different macrophage polarization states. ONEWAY ANOVA and Tukey's multiple comparisons test was applied, and statistical significance is represented by * ($p < 0.05$). Reproduced with permission from Nanomedicine Nanotechnology, Biol. Med, [78]. Copyright 2023, Elsevier Ltd.

in the bloodstream, as well as passive targeting and longer plasma circulation. LNCs possess a semi-rigid shell that facilitates the insertion of amphiphilic molecules onto their surface. Kim and his coworkers achieved active targeting by binding ligands to the surface of LNCs [98]. To produce long-circulating LNCs, researchers inserted the polyethylene glycol distearoylphosphatidylethanolamine conjugate into the LNC shell [99]. Research has demonstrated that LNCs offer a promising approach to overcome the BBB and resulting in enhancing the bioavailability of drugs in the brain [100]. Some of the LNCs used in glioblastoma management are listed in Table 3 [101–108].

3.2.2. Exosome vesicles in GBM therapy

Extracellular vesicles (EVs) facilitate intercellular communication between adjacent and distant cells [109]. Generally, EVs consist of three components: (i) apoptotic bodies, released by cells through programmed cell death and measuring 500 to 1000 nm in diameter; (ii) microvesicles, measuring 150 to 500 nm in diameter; and (iii) exosomes, originating from cells and isolated from bodily fluids, measuring 30 to 120 nm in diameter [110].

3.2.2.1. Exosome isolation strategies. Currently, there are several isolation strategies for the exosomes available and are discussed in the following subsections.

Ultracentrifugation (UC) is the most popular way to isolate EVs from biofluids and cell culture supernatant. Multiple centrifugations at high speeds remove dead cells, debris, and pelleted EVs. Théry et al. presented EV isolation methodology in 2006. Researchers pelleted large EVs at 2000 g, MVs at 10,000 g, and EXOs at 100,000 g and higher. Finally, pelleted EVs were washed by resuspension and pelleted EVs. Fig. 7, I illustrate the concept of UC for exosome purification. Multiple centrifugations at increasing speeds remove large dead cells and detritus; at each stage, the pellet was discarded and the supernatant was used for the subsequent step. The final supernatant was ultracentrifuged at 100,000 g to pellet exosomes and washed the pellet in a large volume of PBS to remove contaminating proteins, and finally centrifuged it again at high speeds [111]. Further, the density gradient flotation (DG)

method was developed to purify isolated EVs, where it primarily removes co-purified non-EV/EV fragments by floating EVs on a gradient of sucrose or iodixanol solutions, which maintain the equilibrium density for exosomes. Harmful stresses during high-speed centrifugation may have reduced the functionality of EVs separated by UC. Following are the common DG steps: Firstly, place layers of a biocompatible medium, such as iodixanol/sucrose, with varying densities to cover the particle densities of the sample in a tube whose densities decrease from bottom to top (Fig. 7, IIA). After adding the material to the density-gradient medium, it is centrifuged for a lengthy time (e.g., 100,000 $\times g$ for 16 h). Isopycnic EVs like exosomes, apoptotic bodies, and protein aggregates end up in the same density layer. Protein clumps settle to the bottom of the centrifuge tube, but exosomes persist in the middle layer at 1.10–1.18 g mL⁻¹. The moving-zone UC features a medium with a density lower than that of all solutes in the sample (Fig. 7, IIB). The DG method allows to isolate vesicles of similar densities with varied sizes, i. e., exosomes, viruses, and large microvesicles. Consequently, the centrifugation time must be carefully determined for optimal exosome isolation, and to minimize exosome pelleting, a high-density medium is normally loaded in the bottom of the centrifuge tube to serve as a cushion.

Recently, researchers have designed various streamlined and easy-to-use ultrafiltration (UF) devices to quickly produce exosomes with yields equivalent to UC. Fig. 7, IIIA, illustrates the process of two tandem-configured microfilters that have size-exclusion limits of 20–200 nm. The 200-nm membrane retains large vesicles, including apoptotic bodies and most microvesicles, while the 20-nm microfilter retains 20-nm vesicles at the bottom and allows proteins to pass through. However, sequential UF is another prominent exosome separation approach (Fig. 7, IIIB). This mode removes cell debris, cells, and apoptotic bodies from extracellular fluids using a 1000-nm filter. The 500-kD MWCO was used to refilter the filtrate, getting rid of free proteins and other small particles. Then, a 200-nm filter was used to separate the 50–200-nm exosomes from the filtrate.

A user-friendly alternative to dUC and DG is size exclusion chromatography (SEC), which does not affect EVs integrity, but preserving

Table 2
Different liposome nanocarriers and their effects in the drug loading.

S. no.	Liposome nanocarriers	Drug loading	Effect	Reference
1	sHDL Nanodiscs	Chemotherapeutic agent: Docetaxel (DTX)	Delivery of DTX-sHDL-CpG nanodiscs into the tumor mass elicits tumor regression and anti-tumor CD8 ⁺ T cell responses in the brain TME. No side effects observed. Further, combination of DTX-sHDL-CpG treatment with radiation (IR) resulted in tumor regression and long-term survival	[82]
2	SPIONS encapsulated in SLNPs	Anti-tumor compound: Nutlin 3a	Magnetic NPs are able to guide the drug to target specific area which act as a powerful inhibitor of cancer cell proliferation while harming their viability.	[83]
3	Lipid based magnetic vectors	Chemotherapeutic agent: TMZ	TMZ-loaded LMNVs demonstrated great anticancer performance	[84]
4	Lipid-based Cubosomes	Drug: AT101	Penetrate into tumor spheroids, show cytotoxic effects against GBM cells	[85]
5	terpolymer-lipid-hybrid nanoparticle	DOX	Enhanced anticancer efficacy and GBM penetration and accumulation.	[86]
6	Cubosomes loaded with miR-7-5p	Chemotherapeutic agents: DOX and TMZ	NPs-loaded with both miRNA and the drug produced an enhanced anti-tumor effect	[87]
7	HA-conjugated LNPs (HALNPs)	DOX	Specifically target GBM Cells over other brain cells due to higher expression of CD44 in tumor cells, resulted in lysosomal evasion and increased efficacy of drug and decreased antineoplastic potency.	[88]

its functionality. The SEC column contains tiny porous polymer beads (the stationary phase), which allow tiny particles from the fluid to penetrate. Thus, bigger particles pass along the column faster and elute earlier. Researchers who study EVs often use SEC as a simple way to deal with UC problems like vesicle rupture and aggregation. Molecules with various hydrodynamic radii behaved differently in a porous stationary phase. Larger molecules, unable to enter the stationary phase pores, push around the porous particles and elute sooner from the column (Fig. 7, IV). These fine, porous materials, like dextran polymer (Sephadex), agarose, and polyacrylamide (Sephacryl or BioGel), have made

SEC the best isolation method over the last 50 years. Especially in the last decade, researchers have developed commercial exosome isolation SEC kits such as qEV (iZON) and PURE-EVs (Hansa Biomed). SEC maintains the biological activity of isolated exosomes, making it more convenient in the biomedical research field. Additionally, SEC uses passive gravity flow, which is better than UC and UF methods as it doesn't damage the vesicles. SEC uses appropriate elution buffers (e.g., PBS) with physiological osmolarity and viscosity, which enhances exosome integrity and the ability of SEC columns to separate highly purified, consistent, and repeatable exosomes. SEC is a time saving approach using selective porous materials and buffer systems, which can be completed within 15 min. Similar to the UF method, the SEC can also employ small-pore manipulation of materials and yield a specified subset of EVs. In comparison to UF, the contact-free method of SEC eliminates sample loss and maximizes yield.

Polymer precipitation strategy is commonly employed to isolate exosomes from biological samples such as blood, cell culture media, CSF, urine, and ascites is to use PEG, which has a molecular weight of between 6000 and 20,000 Da. By removing large impurities such as cell debris and apoptotic bodies, the samples undergo overnight incubation with PEG solution at 4 °C. After precipitation, exosomes were collected using low-speed centrifugation (1500 ×g) and requires no special tools and yields excellent results (Fig. 7, V). Immunoaffinity-ligand-based interactions use various protein markers, antibodies, and exosome receptors to effectively isolate exosomes. Researchers have previously studied abundant exosome markers, including heat shock proteins, platelet-derived growth factor receptors, fusion proteins, lipid-related proteins, and phospholipases. It is better to use biomarkers to isolate exosome subpopulations of different origins, which involves adhering antibodies to a solid surface. Most often, researchers use submicron-sized magnetic particles for immunoprecipitation of recombinant proteins (Fig. 7, VI). The wide surface and near-homogeneity features of this method make it more sensitive and efficient, and the large initial sample volumes can alter the size of the samples for different purposes. Note that disease-specific antibodies and magnetically induced cell sorting can identify disease-specific markers on isolated exosomes. Recently, microfabrication technologies design lab-on-a-chip-style microfluidic devices, which can effectively isolate exosomes. These tiny microfluidic devices can isolate exosomes precisely from body fluids and exploit them in real-time for diagnostic purposes (Fig. 7, VII). Microfluidic approaches are revolutionizing exosome-based diagnostics by combining exosome isolation and characterization into a single step, which is advantageous for non-invasive diagnosis i.e., early-stage cancer screening.

3.2.2.2. Exosome-based theranostics in GBM. Due to their endogenous origin and excellent biocompatibility, exosomes have lower immune clearance and cytotoxicity than pristine NPs. Through their multivalent presentation of cell-driven surface moieties (Fig. 8), exosomes can transport both hydrophilic and hydrophobic drugs across the BBB and target tumor sites [112,113]. In general, exosomes include lipids, proteins, RNAs, and DNAs; most exosome lipids are plasma membrane lipids. These include phosphatidylserine, cholesterol, and sphingomyelin [114]. There are many types of proteins in exosomes, such as heat shock proteins (HSP70 and HSP90), integrins, tetraspanins (CD63, CD81, and CD82), ESCRT complex, Alix, TSG101, and more [115–117]. These proteins help the exosomes form and move through the cells. Exosomes express several proteins on their surface, which interact with recipient cell surface receptors to initiate intracellular signaling. Table 4 summarizes various methods for drug loading using exosomes, highlighting their respective merits and demerits [117–129].

Researchers developed genetically engineered exosome-camouflaged nanocatalysts (Mn@Bi₂Se₃@RGE-Exos) as a biomimetic method. This method made it easier for nanocatalyst enzymes to work better, target glioma cells, and get through the BBB, which improved treatment for GBM. RGE-genetically modified exosomes concealed a

Table 3
Different lipid nanocapsules and their effects in the drug loading.

S. no.	LNCs	Drug loaded	Effect	Reference
1.	Lipid nano capsules	cannabidiol (CBD)	Specifically targeted glioma cells and showed enhanced antitumor affect	[101]
2.	Lipid nano capsules	Anticancer agent: sorafenib (SFN) (a tyrosine kinase inhibitor).	Inhibited angiogenesis and can potentially be used to enhance the efficacy of chemotherapy or RT for treating GB	[102]
3.	lipid nano capsules hydrogel	Chemotherapeutic agent: Gemcitabine, Paclitaxel	Showed increased cytotoxic activity and better antitumor efficacy against GBM	[103]
4.	poly(ϵ -caprolactone) lipid-core nano capsules	Methotrexate	Able to cross the BBB and be captured by cancer and immune brain cells by different mechanisms & is responsible for the higher efficacy of oral MTX-LNC treatment in GBM.	[104]
5.	ϵ -caprolactone nano capsules and lipid nano capsules	Ferrocenyl-tamoxifen derivatives phester and succester	Targets are active against GBM and breast cancer cells	[105]
6.	Chitosan-lipid nano capsules	anti-Galectin-1 and anti-EGFR siRNA	<ul style="list-style-type: none"> Decrease in EGFR and Galectin-1 expression. Induce anti-tumor effects in GBM. Versatile targeted delivery of TMZ against GBM resistant cells. 	[106]
7.	Lipid nano capsules loaded with Marrow-isolated adult multilineage inducible" cells (MIAMI cells)	Ferrociphenol or Fc-diOH	<ul style="list-style-type: none"> High cytotoxicity. New treatment strategy for malignant gliomas. 	[107]
8.	Lipid nano capsule	3,3'-Diindolylmethane (DIM) a phytochemical with antitumor, antioxidant, and anti-inflammatory effects.	<ul style="list-style-type: none"> Nanoencapsulation promoted a sustained release of the bioactive compound in comparison to its free form. Prolonged DIM release and a superior cytotoxic effect against human GBM 	[108]

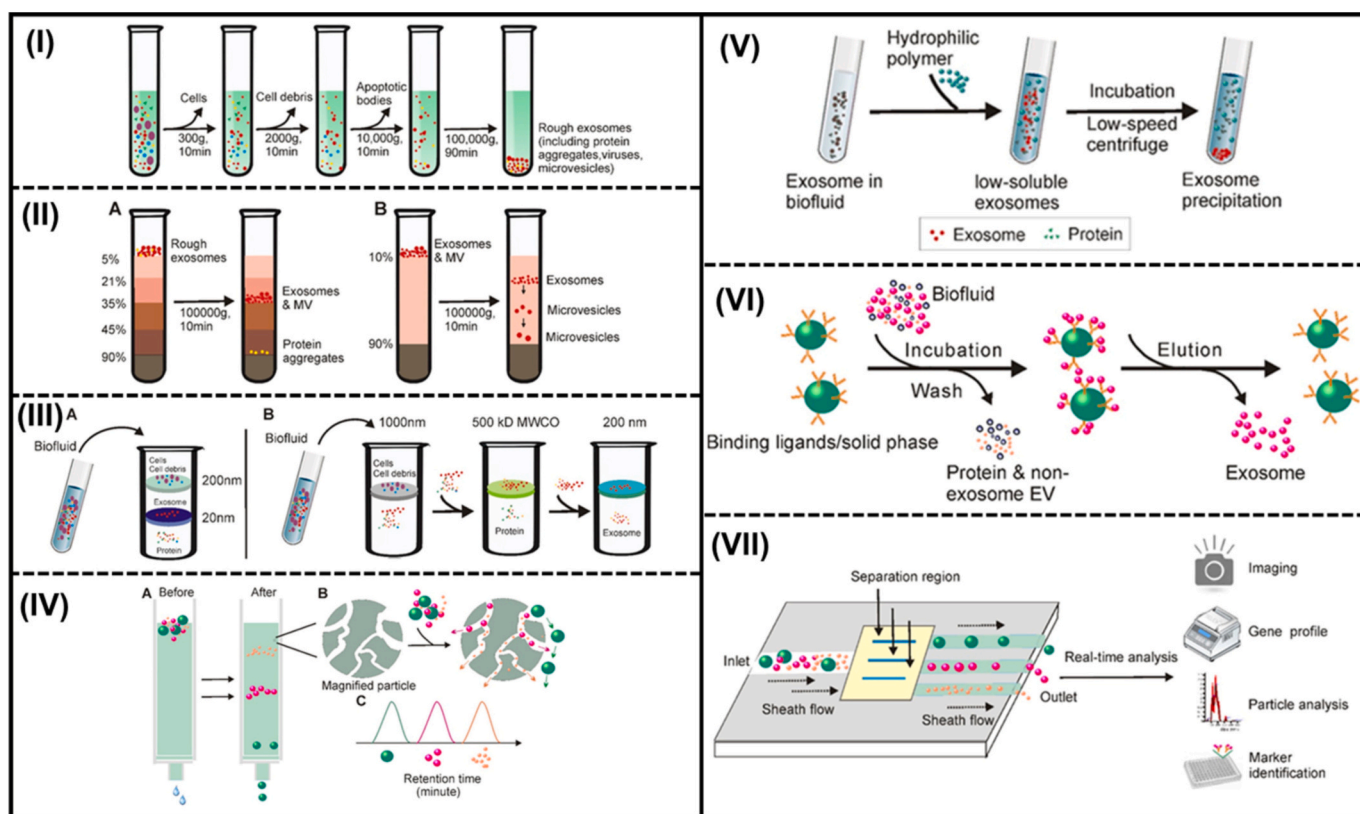


Fig. 7. (I) Schematic representation of different exosome isolation strategies (I) differential ultracentrifugation; (II) gradient density ultracentrifugation, (A) Isopycnic density-gradient ultracentrifugation and (B) The moving-zone gradient ultracentrifugation normally consists two gradient medium sections; (III) ultrafiltration-based exosome separation. (A) tandem- configured microfilter and (B) sequential ultrafiltration; (IV) Size-exclusion chromatography (A) When passing a solution through a stationary phase consisting of porous resin particles, molecules can be separated according to size and (B) While particles with hydrodynamic radii smaller than that of the pores of the stationary phase enter into the pores for longer traffic distance, larger particles, which cannot enter the pores move directly around the resin; (V) Polymer Precipitation Strategy; (VI) immunoaffinity-based capture; and (VII) Integrated microfluidic technique. Reproduced with permission from Theranostics [111], Copyright 2020, Ivyspring International Publisher.

single Mn atom anchor within Mn@Bi₂Se₃@RGE-Exos. RGE-peptide-modified exosomes were able to penetrate glioma cells and adhere to them. When put in contact with an NIR-II 1064 nm laser, the biomimetic nanocatalysts sped up the process of changing H₂O₂ into ·OH, ¹O₂, and

O²⁻. The photon-activated nanozyme-catalyzed cascade reaction threw off the balance of cells, boosted the immune system, and caused ferroptosis to kill cancer cells. Thus, this biosafe GBM anticancer treatment has enormous potential. This strategy is a promising model for NIR-II

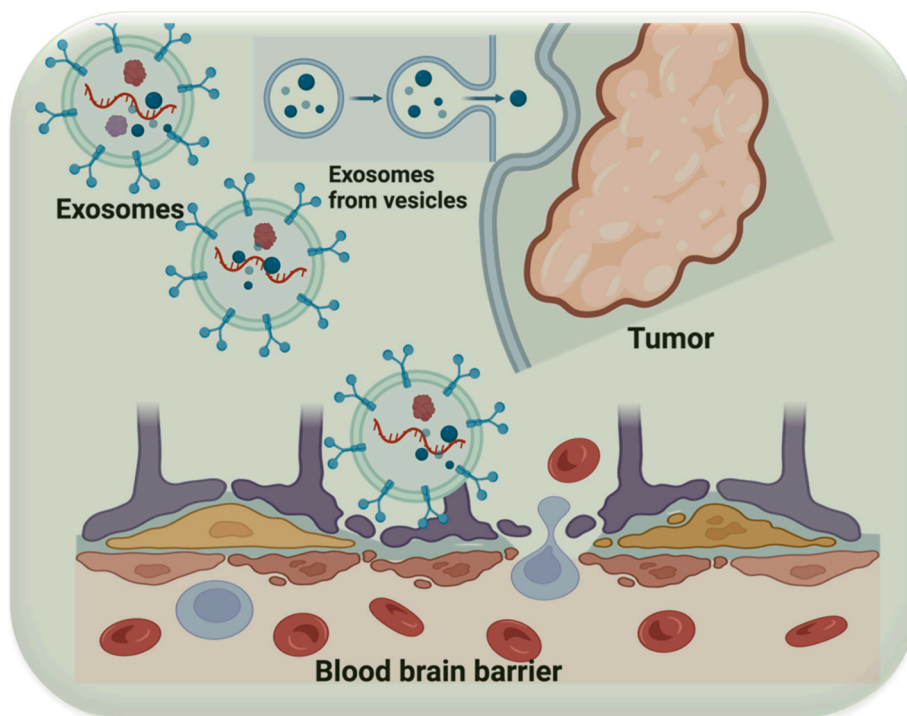


Fig. 8. Role of exosomes in GBM via crossing BBB.

light-driven bio-nanocatalysis against GBM [130]. Researchers have studied Prussian blue NPs (PBNPs) for photoacoustic imaging (PAI) and PT ablation. Glioblastoma therapy restricts their use due to their inability to penetrate the BBB. Researchers demonstrated that they can use a hybrid biomimetic nanoparticle, consisting of PBNP and an exosome from U-87 cancer cells (Exo:PB), to treat brain tumors using heat. Significant photoconversion makes this possible. Particle analysis revealed an exosome-marked covering surrounding PBNPs. In vitro U-87 exosome uptake patterns are identical to native ones, and an 808 nm laser causes localized cell death. Glioblastoma mice receive Exo:PB through an IV, which targets and eliminates more tumor volume than PEG-coated PBNPs. Unlike RGD:PB, Exo:PB demonstrated preferential tumor accumulation and minimal off-targeting. Covering the tumor with Exo:PB and staining it with H&E and Ki67 in studies done outside of living organisms showed accurate targeting. The above-mentioned biomimetic nanocatalyst can naturally cross the BBB and act as a therapeutic agent for systemic glioblastoma tissue targeting and PTT [131].

In this context, neuron-derived exosomes from culture mediums contain abundant miRNA and short RNAs. Neuronal identity and function depend on high miR124-3p levels. Exosomes can deliver neuron-specific miRNAs to astrocytes and other glial cells. Exosomes from the T98G GBM cells contain higher levels of L1CAM proteins, linked to the development of gliomas. L1CAM proteins regulate neuronal differentiation and migration throughout normal development. This study found that more IFN-gamma, IL1A, IL12, IL1B, IL8, CXCL10, and complement factor C5 were present in the exosomes of human astrocytes from GBM. These exosomes produce various pro-inflammatory chemokines and interleukins, including CSF2 and 3, IL4, IL10, and IL13, which can control T cells and weaken the immune system through immunosuppression (Fig. 9, I) [132]. Researchers have studied tumor-derived exosomal miRNAs as serum and CSF glioma biomarkers, using them to monitor radiation response and recurrence, and have suggested the therapeutic potential of exosomes in liquid biopsy. Zeng and his colleagues discovered that TMZ-resistant GBM cells produced exosomes with reduced miR-151a levels in CSF [133]. TMZ sensitivity increased after cell transfection restored miR-151a levels. Further, Lan et al. found that GBM patients have higher tumor-derived serum exosome miR-301a

than healthy controls in 2018. Exosome miR-301a was associated with tumor grade, declined Karnofsky performance score (KPS), and recurrence. Researchers led by Mantolera et al. found serum exosomes from 50 people with GBM and 30 healthy controls. They found big differences in the amounts of miR-574-3p, miR-320, and RNU6-1 genes (Fig. 9, IIa) [132,134]. Further, Xu and his coworkers demonstrated that miR-133b-loaded mesenchymal-stem cell exosomes inhibited glioma development [135]. Glioma-derived exosomes upregulate miR-21, miR-222, miR-9, miR-10a, miR-R124-3p, miR-124b, miR-221, miR-103, miR-302-367, miR-124a, miR-1246, and miR-1290. Genetically modified MVBs can bundle mRNA, proteins, and drugs into exosomes, making them effective for immunotherapy. Zhuang et al. injected exosomal curcumin and JSI124 (i.e., Stat3 inhibitor activator) into the brains of rodents through the nose. Intranasal exosomal-encapsulated curcumin restricted GL26 glioma cell proliferation (Fig. 9, IIb) [132,136]. Moreover, from the last decade, researchers have identified multiple miRNAs, proteins, and long non-coding RNAs (lncRNAs) from glioma exosomes, which are linked to progression, invasiveness, viability, and angiogenesis of glioma. Katakowski and his colleagues isolated exosomes from stromal cells of bone marrow to generate a rat model of a primary brain tumor called miR-146b, which lowers EGFR expression, thereby drastically reducing tumor cell proliferation, and significantly fights against gliomas [137]. McDonald et al. used exosomes to deliver a number of glioma-specific miRNAs to stem cells, which include miR-124-2, miR-135-2a, and let-7i had the most anti-GBM activity across different types of GBM [138]. Further, a broad list of recently used exosomes utilized in GBM is summarized in Table 5 [139–144].

3.2.3. Silica nanoparticles

Silica NPs (SiNPs) have a number of advantages that make them popular in medical applications, including superior biocompatibility, a wide surface area for drug loading, stability, and low cost. The potential of SiNPs to kill cells, damage DNA, and generate ROS has hindered their use as biomarkers, cancer treatments, or DDSs [145,146]. Various fields have since studied SiNPs for their clinical safety and potential applications. Because proper size, dosage, and cell type can control SiNP toxicity, researchers can now explore multimodal SiNP adjustments to

Table 4

Different strategic methods of loading different therapeutic molecules into exosomes and their advantages and disadvantages.

S. no.	Method	Advantages	Disadvantages	Reference
1	Incubation with drugs (passive loading method)	<ul style="list-style-type: none"> Simplest method. Increasing solubility and stability of the hydrophobic drugs in blood circulation. 	<ul style="list-style-type: none"> Low drug-loading efficiency. Not efficient for large Molecules. 	[117,118]
2	Electroporation (active loading method)	<ul style="list-style-type: none"> Loading with large molecules are possible. Applicable for nucleic acids. 	<ul style="list-style-type: none"> Low drug-loading efficiency (hydrophobic drugs). Cargo aggregation. 	[119,120]
3	Sonication (active loading method)	<ul style="list-style-type: none"> High drug-loading efficiency. Applicable for nucleic acids. 	<ul style="list-style-type: none"> Deformation of membrane. Low drug-loading efficiency (hydrophobic drugs). 	[121,122]
4	Extrusion (active loading method)	High drug-loading efficiency.	<ul style="list-style-type: none"> Deformation of membrane. Limitation of membrane. 	[123]
5	Freeze and thaw cycles (active loading method)	<ul style="list-style-type: none"> Fusion of membranes possible. 	<ul style="list-style-type: none"> Low drug-loading efficiency. Exosome aggregation. 	[123,124]
6	Click chemistry (active loading method)	<ul style="list-style-type: none"> Quick and efficient reactions. High specificity. 	<ul style="list-style-type: none"> Impairing the functionality of surface proteins. 	[125]
7	Mimetic Nanovesicles (exosome-mimic)	<ul style="list-style-type: none"> Easier to manufacture. High therapeutic delivery efficiency. High yield production. 	Required to understand cargo loading (cellular uptake, cargo release, and fate of vesicles)	[126–129]

make them practically useful [147]. Synthetic modification of SiNPs can alter the increased toxicity of smaller-sized SiNPs [148]. Transferrin-modified porous silica NPs are a popular way to treat GBM right now because they are biocompatible, biodegradable, and can hold drugs. The BBB and GBM cells often had too much of the transferrin receptor on their surfaces. This means that transferrin-functionalized SiNPs can help the DOX stay where it needs to be for longer. A low-power radio-frequency field, featuring a mesoporous silica shell and an iron oxide core with fibronectin-targeting ligands on the outside, made this possible. As a result, SiNPs could effectively deliver drugs on a large scale and throughout the GBM [149–151].

Generally, traditional indocyanine green (ICG) PT agents are not very stable; they are only available in the bloodstream for a short time and cannot easily enter the brain due to the BBB's obstruction, which makes them less effective in treating GBM. In this context, Sun and his colleagues have designed innovative SiNPs-based nanoprobe for GBM PTT, which circumvent the BBB. G-ICG-SiNPs, composed of glucosamine (G), ICG, and glucose transporter-1 (GLUT1), possess the ability to effortlessly cross the BBB, penetrate mice's brains, and accumulate at GBM sites. After 25 days of storage, G-ICG-SiNPs loaded with the same dose of ICG decayed by 34.6 %, while ICG decayed by 99.5 %. Compared to ICG, G-ICG-SiNPs exhibited 17.3-fold longer blood circulation times. They required 5 min of 808 nm NIR light to heat the GBM surface to

45.3 °C, while the ICG group only reached 36.1 °C under the same conditions. The above-mentioned excellent stability and longer blood circulation time features make G-ICG-SiNPs superior PT agents in GBM therapy [152].

3.2.4. Polymeric nanoparticles

PNPs are solid, colloidal drug delivery tools made of biocompatible, hydrophobic polymers or copolymers, which can be natural or man-made and have diameters between 1 and 1000 nm. There are several ways to load drug moieties into PNPs. The NP matrix can hold them in position, whether they are solid or in solution, as long as the PNP core is liquid, covalently bonded to the polymer, or adsorbed on the particle surface. They can entrap tiny pharmacological molecules that are both hydrophilic and lipophilic, as well as macromolecular drugs. Based on the type of final formulation, researchers primarily divide PNPs into two groups: nanospheres and nanocapsules. The chemical structure of the polymers used to prepare PNPs allows for a wide range of medicinal applications, which can deliver numerous drugs to the brain. Nanospheres, composed of a polymer matrix, which can dissolve or adsorb drug molecules on the particle surfaces. Similar to vesicles, nanocapsules dissolve drugs in a liquid core, separated by a polymer membrane [153–155].

3.2.5. Carbon quantum dots and carbon nanotubes

Li et al. made LAAM CQDs, which are similar with amino acids and constitute α -carboxyl and amino groups paired on their edges and they can interact with LAT1 in many ways. These LAAM CQDs were successfully crossed the BBB, gathered at brain tumors, and responsible for the strong NIR fluorescence in living organisms. Furthermore, LAAM TC-CQDs with large π -conjugated structures may effectively move chemotherapeutic drugs that damage DNA by stacking them on top of each other. TPTC-loaded LAAM TC-CQDs specifically killed more U87 cells than free TPTC due to their selective accumulations in tumors and a long-duration half-life [156]. Nanomaterials that are atomically thin can improve electronic transfer, band structure, and optical properties by interacting with heteroatoms. Black phosphorus quantum dots (BP QDs) are considered convenient theranostic agents due to their natural biocompatibility and strong photochemical effects. However, BP QDs are not competitive regarding NIR-II window medical diagnosis and X-ray-induced phototherapy. Researchers designed Nd^{3+} ion-coordinated BP QD (BPNd) to improve its performance in NIR-II fluorescence imaging and X-ray-induced PDT. Because of their small size, BPNds can easily cross the BBB to precisely track the growth of glioblastoma through intracranial NIR-II fluorescence imaging and stop its progression with specific X-ray-induced, synergistic PD-based chemotherapy [157]. Most dual nanodrug delivery systems fail to infiltrate malignant brain tumors due to poor targeting and nanoparticle size growth after drug conjugation. The authors employed carbon dots (C-dots) with an average particle size of 1.5–1.7 nm to create a triple conjugated system. There are three different kinds of particles in this system. The smallest particles, measuring about 3.5 nm, consist of C-dots, transferrin, the targeted ligand, and two anti-cancer drugs, epirubicin and temozolomide (TMZ). Researchers studied glioblastoma brain tumor cell lines SJGBM2, CHLA266, CHLA200 (pediatric), and U87 in vitro. Further, investigated the performance of the triple conjugated system (dual drug conjugation with transferrin) in contrast to the single drug conjugation, C-dots drugs without transferrin, and free drug combinations. Even at low concentrations, transferrin-conjugated samples had the lowest cell viability. The triple conjugated system (C-dots-trans-temo-epi (C-DT)) proved more cytotoxic to brain tumor cell lines than dual conjugated systems. C-DT raised cytotoxicity in SJGBM2 to 86 % at 0.01 μM , while C-ET and C-TT decreased it to 33 and 8 %, respectively. Triple-conjugated C-DT increased cytotoxicity, and the two-drug combination synergized [158].

Researchers are using new boron-containing carbon dots (BCDs) for boron neutron capture treatment (BNCT) to track 10B in both in vitro

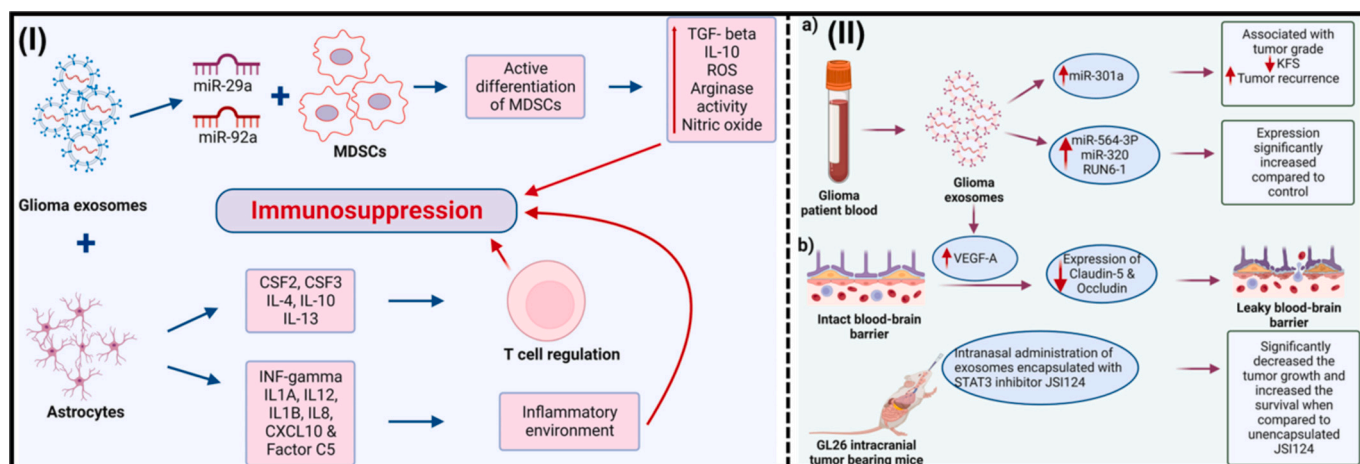


Fig. 9. (I) Exosome-mediated cellular crosstalk between tumor cells, astrocytes, and immune cells in the glioma tumor microenvironment drives immunosuppression. Glioma-derived exosomes contain miR-29a and miR-92a, which promote the differentiation of MDSCs and enrich TME in immunosuppressive factors. Astrocytes release multiple signaling factors, which promote an anti-inflammatory environment and inhibit T-cell activity. TME, tumor microenvironment; MDSCs, myeloid-derive suppressor cells; (II) Exosomes serve as a biomarker and drug carrier. a) Utility of glioma-derived exosomes in serum-based liquid biopsy for detecting tumor recurrence, decreased KPS, and elevated tumor grade. b) Example of exosome utility as drug delivery vehicles for glioma therapy in a murine model. Delivery of exosomal curcumin and JS1124 (a signal transducer and activator of stat3 inhibitor) to the rodent brain via intranasal injection. KPS, Karnofsky Performance Score. Reproduced with permission from Cancer Letters, [132]. Copyright 2024, Elsevier Ltd.

Table 5

List of currently employed exosomes used in the GBM therapy.

S. no.	Exosome used in treating glioma	Effectiveness in treating glioma	References
1.	Natural killer-exosome	<ul style="list-style-type: none"> Exerted antitumor effects on glioblastoma cells both in vitro and in vivo. Helpful in treating incurable GBM. 	[139]
2.	Exosomal lncSBF2-AS1	<ul style="list-style-type: none"> GBM cells remodel the tumor microenvironment to promote tumor chemotherapy-resistance by secreting the oncogenic lncSBF2-AS1-enriched exosomes serve as a possible diagnostic marker for therapy-refractory GBM. 	[140]
3.	Exosome-coated DOX-loaded NPs	<ul style="list-style-type: none"> Could penetrate the BBB both in vitro and in vivo. ENP_{DOX} induced apoptosis and ICD of glioma GL261 cells. Systemic administration of ENP_{DOX}. This resulted in maturation of dendritic cells, activation of cytotoxic cells, altered production of cytokines, suppressed proliferation, and increased apoptosis of GBM cells in vivo. Prolonged survival of GBM-bearing mice. 	[141]
4.	miR-21-sponge exosome	<ul style="list-style-type: none"> Decline in proliferation and also an elevation in apoptotic rates. Exosomes loaded with a miR-21-sponge construct led to a significant reduction in the volume of the tumors in a rat model of GBM. 	[142]
5.	hEnMSCs-derived exosomes loaded with atorvastatin	<ul style="list-style-type: none"> Mimicked the anti-tumor effects of free atorvastatin. Also potentiated its anti-tumor effects on GBM. 	[143]
6.	GBM-derived exosomes loaded with selumetinib	<ul style="list-style-type: none"> Specific antitumor effect on U87MG human GBM cells. Non-toxic to healthy brain cells. 	[144]

and in vivo, which are highly water soluble and possess better optical properties. Encapsulating BCDs with macrophage exosomes (Exos) results in ≈ 100 nm BCD-Exos. Using fluorescent U-87-MG glioma cells to image the tumors showed that BCD-Exos was taken up, crossed the BBB, and gathered in the tumors of mice with orthotopic U-87-MG glioma 4 h after treatment. The amount of 10B in tumor tissue is 107.07 ± 1.58 ppm, according to ICP-MS research. The T/N ratios increase from 2.03 ± 0.08 for BPA to 5.28 ± 0.29 for BCD-Exos. The neutron radiation dose in BNCT is 8.40 ± 0.12 Gy at 500 mg kg^{-1} 10B dosage. Final results show that BCD-Exos-treated brain glioma has a strong BNCT effect in mice, and the survival rate is 100 %. BNCT is a beneficial way to treat brain gliomas because it can change where boron is located in cancer cells, raise the T/N ratios, and use fluorescence imaging to show exactly where boron and neutrons are interacting at the tumor site [159]. Perini and his co-workers employed three GQDs with distinct surface chemical functionalizations: green GQDs with no surface-specific functionalization, COOH-GQDs, and NH₂-GQDs. The combined action of GQDs and Dox on U87 cells showed a synergistic effect on cell viability. GQDs' membrane alteration ability is associated with their improved in vitro effectiveness on glioma cells. Cortical neurons did not exhibit a similar synergistic effect. We also demonstrated a strong connection between membrane fluidity and the surface charge of the three GQDs, as well as the permeabilization of cells by distinct GQDs. The way that GQDs and chemotherapy drugs work together biophysically can help us make a new way to deliver drugs that can cross the BBB [160].

Carbon nanotubes (CNTs) can convert NIR light into heat, making them a promising drug delivery and cancer therapy method. Carbon allotropes typically yield two types of CNTs: single-walled carbon nanotubes (SWNTs) and multi-walled carbon nanotubes (MWNTs). Researchers found that GBM cells treated with anti-CD133 monoclonal antibody-conjugated SWNTs under NIR laser light has demonstrated promising results for GBM therapy [161–163].

3.3. Cell membrane-camouflaged nanoparticles

CMCNPs are being considered biomimetic materials because their surfaces resemble CMs, and further modification can enhance their performance. Researchers often design CMCNs by combining core NPs and CMs through a porous polyester or polycarbonate membrane with different hole diameters. Because NPs are fluidic, mechanical extrusion drives them through membranes and produces them with a uniform size

distribution and minimal protein denaturation. Many researchers would rather use sonication than extrusion because the ultrasonic cavitation bubbles can break through the membrane structure and rebuild the core NPs by co-incubating vesicles around them. Fine-tuning the power, frequency, and duration of sonication improves coating dispersion and stops material loss, which speeds up fusion and slows down protein denaturation. Additional heat production and unequal morphology are the drawbacks of sonication; thus, researchers must cool membrane proteins to escape the heat sensitivity. With a high electric field, microfluidic electroporation makes holes on CMs that allow core NPs to enter membrane vesicles. In a way similar to sonication, we can change the pulse voltage, flow speed, and duration to make the method more uniform, stable for colloids, scalable, and useful in biological systems. FDA-approved microfluidic electroporation chips must follow GMP for batch-to-batch accuracy. Finally, electrostatic interaction between positively charged NPs and negatively charged CMs boosts spontaneous CMCNPs production. Tasciotti's CMCNPs absorb both positive silicon NPs and negative leukocyte membrane-derived vesicles simultaneously. Hydrophobic and electrostatic interactions induce spontaneous fusion, requiring precise NP surface charge control. NPs with high positive charge produce an imprecise coating due to strong vesicle interactions. A multilamellar surface may develop if the contact is not powerful enough to break the adsorbed vesicles. Fig. 10 (I) summarizes these methods [32].

The gold standard for characterizing CMCNPs is transmission electron microscopy (TEM) because their inner cores are electron-densely packed at a different density than protein and lipid CMs. CMCNPs are white, spherical core NPs with light-gray rings under TEM. The empty CM-derived vesicles, which break apart to reveal nano-sized ones, show

up as white circles. The spherical NPs inside the cores, on the other hand, stand out very sharply against the background (Fig. 10, IIa). TEM images show NP coatings and core NPs (Fig. 10, IIIb, and b') [164]. In another study, Wu et al. synthesized CMCNPs using poly(lactic-co-glycolic acid), mangostin, and a platelet-C6 hybrid biomimetic coating, which are morphologically similar with the membranes of tumor and platelet cells (Fig. 10, IV) [165]. Further, glioma targeting and anti-cancer efficacy potentials of the CMCNPs were investigated in vitro and in vivo. The biomimetic coating made it easier for nanocarrier active drugs to target and get past the immune system in C6 and THP-1 cells, which made them more dangerous. To explore the intrinsic features of both source cells, β -PCNPs were analyzed. In contrast to bare β -NPs, β -PCNPs demonstrated enhanced tumor targeting and C6 cell death in vitro. In mice, IV delivery via β -PCNPs led to improved tumor targeting and superior glioma tumor growth suppression. Additionally, animals in the β -PCNP group had longer drug circulation times and better outcomes than those in the β -NP group. These findings suggest using PCNPs as drug carriers to improve the efficacy against glioma. Xie and his colleagues constructed a ZIF-8 bioreactor with a CM covering that utilizes DOX and glucose oxidase (GOx) to starve and kill cancer cells. Fig. 10 (V) illustrates the effective loading of DOX, a model anticancer drug, into the ZIF-8 nanostructure (ZD). Then, using a lipid insertion method, the exterior of the RBCm was modified, with the well-known RGD peptide to target cancer. We created the RGD-mGZD bioreactor by extruding the modified membrane and GOx with NPs. The flexible bioreactor recognized the overexpressed integrin receptors on the tumor CM, enabling the body to retain blood longer and direct it to the tumor site, which allowed the nanodrugs to accumulate efficiently. GOx has the potential to swiftly absorb intratumoral glucose and oxygen, thereby

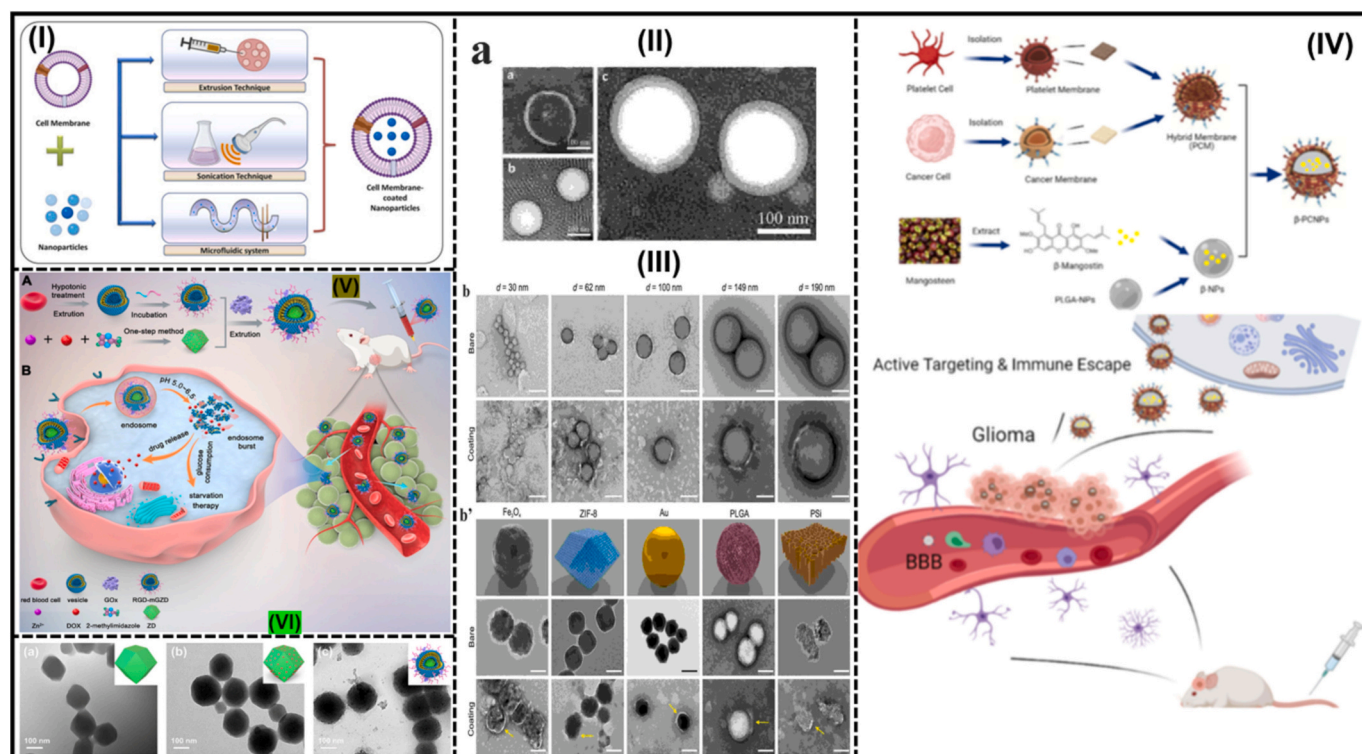


Fig. 10. (I) A pictorial representation of different extrusion techniques used to fuse cell membrane vesicles with nanoparticles; (II) Characterization of nanoparticles coated with cell membranes. a) TEM images of NPs; (III) b) TEM images illustrate nonporous SiO₂ NP sizes before and after cell membrane coating. 100-nm scale bars. b') TEM pictures of Fe₃O₄, ZIF-8, Au, PLGA, and PSi NPs before and after coating with cell membranes. 100-nm scale bars; (IV) Schematic representation for the active targeting and immune escape mechanism by CMCNPs; (V) Schematic Illustration of (A) Preparation of RGD-mGZD Bioreactor and (B) RGD Peptide Modified RBCm Coated ZIF-8-Based Bioreactor for Glioma Targeted Starvation-Chemotherapy; (VI) Characterizations of RGD-mGZD. (A) TEM images of ZIF-8 (a), ZD (b) and RGD-mGZD (c). (I) Reproduced with permission from Journal of Controlled Drug Release, [32]. Copyright 2022, Elsevier Ltd.; (II & III) Reproduced with permission from Nature Communications, [164]. Copyright 2021, Springer Nature Ltd.; (IV) Reproduced with permission from International Journal of Nanomedicine, [165]. Copyright 2021, Dove Medical Press Ltd.; (V) Reproduced with permission from Journal of Colloid and Interface Science, [166]. Copyright 2022, Elsevier Ltd.

starving cancer cells and producing gluconic acid and hydrogen peroxide for treatment. In addition, the tumor's acidic microenvironment may degrade ZIF-8 structure, releasing DOX for enhanced treatment. The developed bioreactor might enhance starvation-chemotherapy's synergistic efficiency by effectively and safely eliminating cancer cells. Fig. 10 (VI) displays the TEM images of the synthesized ZIF-8, ZD, and RGD-mGZD, which reveal an even distribution of sizes at 140, 165, and 200 nm, respectively [166]. Compared to bare NPs, RGD-mGZD displayed a unique core-shell structure, confirming the presence of RBCm coating.

4. Combinatorial nanomedicines; as therapeutic targets in GBM therapy

Despite much research, there is no effective treatment for GBM. Researchers are actively working toward the development of effective and unique treatment techniques for GBM. So far, the standard treatment for GBM is surgical resection, followed by TMZ-based chemoradiotherapy. However, recurring GBM tumors are a common phenomenon, despite full surgical resection and vigorous adjuvant therapy received. Overall, several factors could complicate the treatment of GBM, such as incomplete resection, mild genetic variations, the complexity of the blood-brain barrier, and an environment that weakens the immune system [167,168]. In this regard, combination therapy, which combines one or more therapeutic platforms into a single strategy, has garnered scientific interest among GBM patients. Researchers made a targeted PNPs that deliver anti-miR-21 and miR-124 into the brain to treat GBM effectively [155]. Angiopep-2 targets two different areas simultaneously, enabling the attachment of the Angiopep-2 peptide to PNPs. By forming three types of bonds: electrostatic, hydrogen, and hydrophobic, PNPs can prevent blood enzymes from breaking down miRNA. It can also cross the BBB and deliver miRNAs such as anti-miR-21 and anti-miR-124 together stopped the mutant RAS/PI3K/PTEN/AKT signaling pathway to treat GBM. This synergistic effect showed that miRNA nanomedicines can greatly reduce tumor cell growth, migration, and invasion, as well as the formation of new blood vessels. Further researchers investigated miRNA nanomedicines in an orthotopic GBM xenograft model and found that they effectively slowed down tumor growth and greatly enhanced the median survival time. This showed that PNPs effectively blocked miR-21 and miR-124 supplementation, greatly mitigating tumorigenesis, and thereby suggesting that they could

be useful in treating GBM [155]. Fig. 11 illustrates GBM therapy involving significant drug candidates via various mechanisms.

4.1. Chemotherapeutics in combination therapy

Studies have demonstrated that combinations of two or more therapeutic therapies in GBM outperform monotherapy and chemotherapy. The monotherapy approach does not specifically target fast-proliferating cells, and chemotherapy results in a significant toxicity burden and immunosuppression. GBM is the most common and aggressive brain tumor in adults, with a highly unfavorable prognosis. Despite the identification of new treatment targets in the last decade, monotherapy has proven unsuccessful in clinical studies. Therefore, it is necessary to shift the researcher's focus to combination therapy in the treatment of GBM. Specifically, small-molecule inhibitors have shown enormous potentials to treat GBM. In this regard, few signaling pathways including PI3K/AKT/mTOR pathway, the DNA damage response, TP53, and pathway involving cell cycle inhibitors can be blocked to treat GBM. P-glycoprotein 1 (P-gp1)-TMZ resistance in BBB endothelial cells occurs through an efflux mechanism, and the drug morphine inhibits P-gp1 as well as their combination has shown significant results for treating GBM. Furthermore, lowering the TMZ medication dose lowers chemoresistance, enhancing the long-term therapeutic response [169]. Giving GBM cells (U87 and U251) SGT-53 TMZ and TP53 from outside the tumor through a tumor-targeted nanocomplex (SGT-53) improved the effectiveness of chemotherapy, thereby increasing the average survival time [170]. Transferrin-functionalized NPs (Tf-NPs) have delivered double doses of TMZ and the bromodomain inhibitor JQ1, which is more likely to kill cells and damage DNA. When compared to free-drug dosing, this leads to a 1.5- to 2-fold reduction in tumor burden and enhanced survival [171]. Researchers used SFN to treat TMZ-resistant cell lines (U87-R and U373-R) in chemoresistant xenografts in naked mice; it reversed the chemoresistance, slowed down cell growth, and finally caused cell death. Also, researchers have found that SFN blocks miR-21 through the Wnt/catenin/TCF4 signaling pathway, which makes cells more vulnerable to chemotherapy [172].

4.2. Radiotherapy in combination therapy

RT treats 40 % of malignancies and a variety of tumor types, and its advancements in GBM therapy are significant. The high-Z effect is an

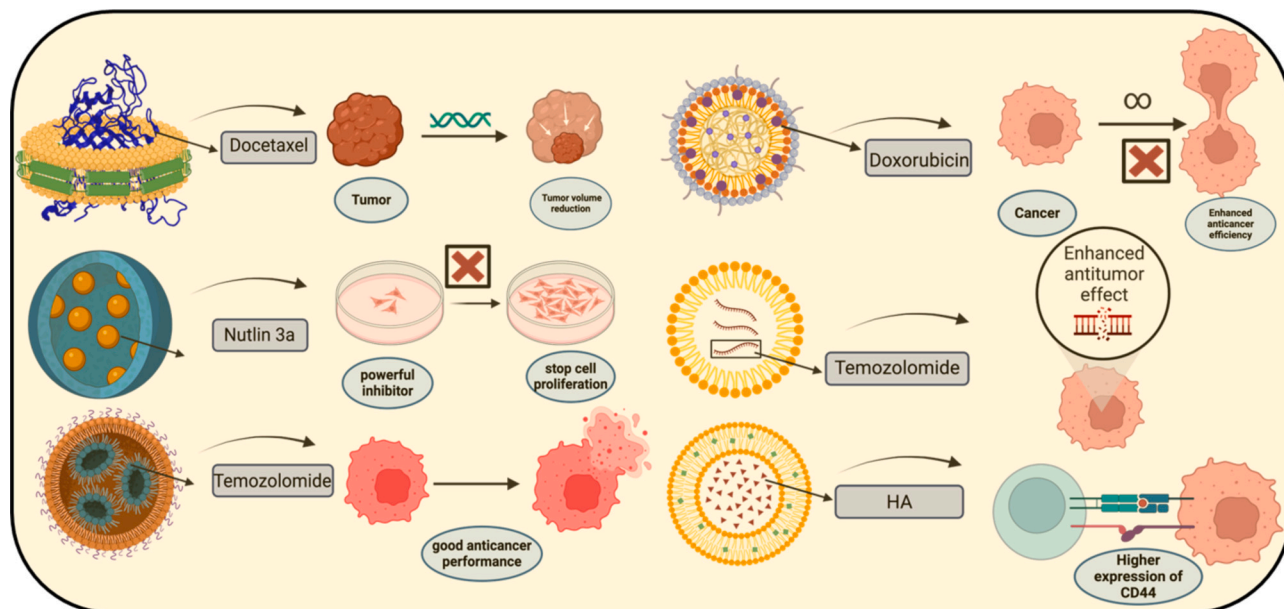


Fig. 11. Overview of different drug candidates for GBM therapy.

important phenomenon that happens when ionizing radiation hits heavy metals with large photoelectric cross sections [173]. It causes a cascade of Auger/Compton electrons, scattered X-rays, and photons. This can boost the effective radiation dosage and destroy GBM tumors. According to 2005 data, GBM treatment comprises radiation, daily TMZ, and maximum safe resection (Fig. 12, I). Due to its invasiveness, GBM recommends postoperative radiation, making complete resection with favorable neurological results nearly impossible. The Brain Tumor Study Group (BTSG) conducted many randomized clinical trials to prove radiation's effectiveness in the 1970s. WBRT improved survival (median 8.4 vs. 3.5 months) in the first clinical trial (BTSG 66–01). The second clinical research (BTSG 69–01) found that WBRT improved survival over optimum supportive care or chemotherapy. To understand high-Z metal NP radiosensitization, two factors must be considered: physical dose augmentation and tissue biological response. The main reason for physical dose augmentation is that high-Z metals block radiation better than soft tissue. High-Z metals induce Compton and photoelectric reactions when radiation impacts matter, accumulating energy in tumorous tissues. Compton scattering involves photons transmitting energy to weakly bound electrons, which then leave their orbits. After losing energy, the incident photon disperses. The photon continues, while the electron ionizes nearby tissue (Fig. 12, IIa). Incoming photon

energy inversely affects Compton interactions, which dominate the 25 keV to 25 MeV photon energy spectrum. Most RTs use energy levels between 6 and 20 MeV, making the Compton effect the main interaction in tumorous tissue. High-Z metal nanoparticles have photoelectric effects that create photoelectrons, secondary photons, and Auger electrons. These photoelectric effects lead to increased dosage and focus cell ionization (Fig. 12, IIb). Most preclinical studies on NPs and RTs have used keV photons to increase their radiosensitization, as the photoelectric effect decreases with increasing photon energy. The radiosensitization of gold nanoparticles causes DNA damage, oxidative stress, changes in the cell cycle, and effects on other cells (Fig. 12, III). Radiation primarily causes cell death by damaging DNA with ROS, which include free radicals such as superoxide ($\cdot\text{O}_2^-$) and hydroxyl ($\cdot\text{OH}$), as well as other oxidative chemical species such as hydrogen peroxide (H_2O_2), singlet oxygen ($^1\text{O}_2$), and hypochlorous acid (HOCl). Radio waves interact with matter to generate electrons and ROS, which cause oxidative stress, DNA breakage, and cell death (Fig. 12, IV). Previous research studies showed that high-Z metal NPs generate substantial ROS and damage DNA, where AuNPs measuring 1–2 nm showed substantial toxicity, with an IC50 value of 30 to 56 μM . The high interactions between high-Z metal NPs and ionizing radiation also accounted for the enhanced ROS generation. Misawa et al.'s research revealed a 1.46-fold

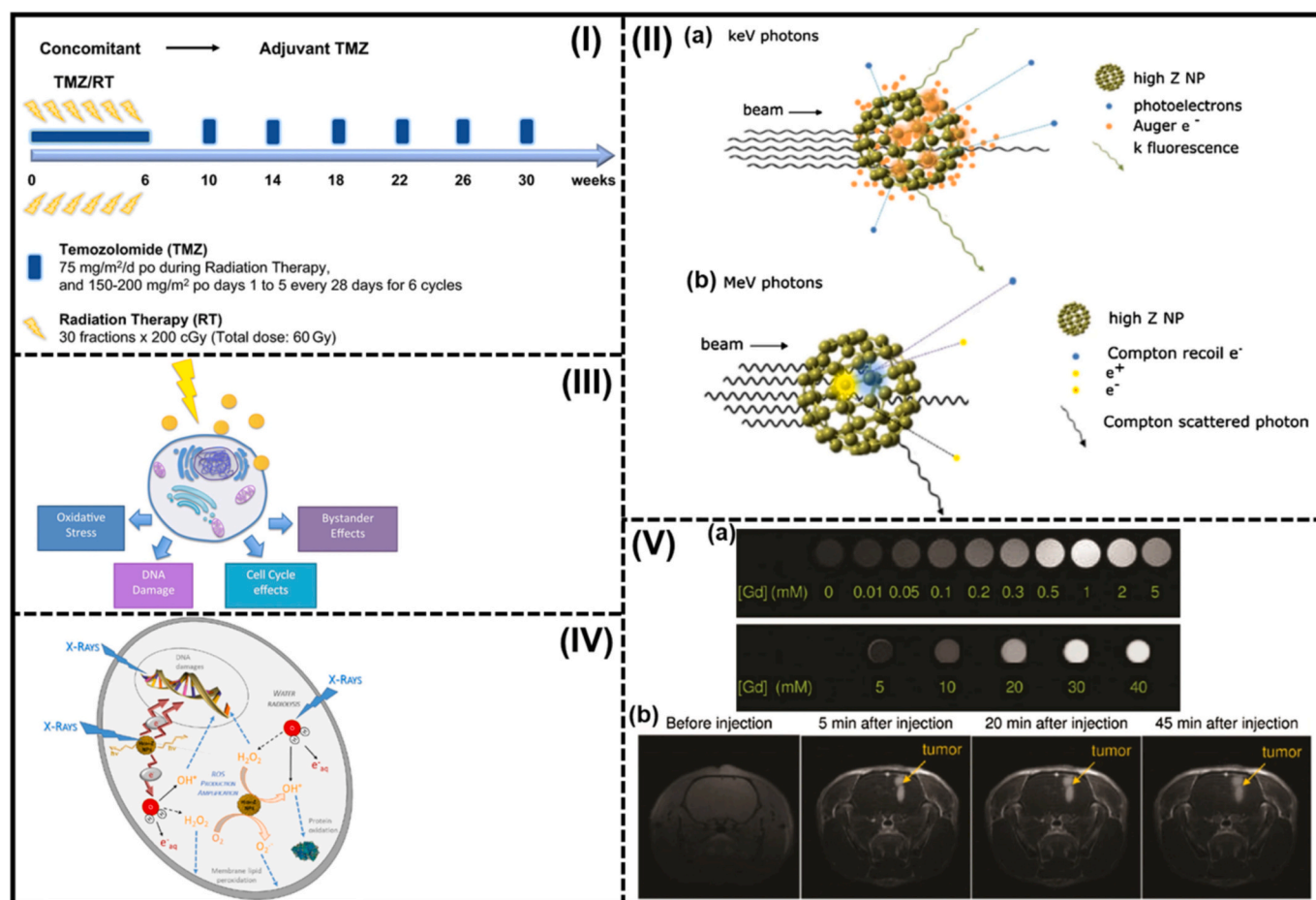


Fig. 12. (I) The schematic schedule of TMZ treatment. This schedule included RT with treatment of TMZ. After the end of 6 weeks RT with TMZ of 75 mg/m²/day, the first of six adjuvant TMZ started. The 6 cycles of adjuvant TMZ was conducted with 150–200 mg/m² po days 1 to 5 every 28 days; (II) Schematic illustration of inelastic interactions with a high-Z nanoparticle for: (a) incident keV photons (orange clouds represent photoelectric events); (b) incident MeV photons (blue and yellow clouds represent Compton scatter and pair production events, respectively); (III) The biological mechanisms of GNP radiosensitization. There are several biological effects involved in GNP: oxidative stress, DNA damage, cell cycle, and bystander effects; (IV) Biological mechanism of interaction between incident photons and high-Z NPs; (V) The survival improvement of brain tumor bearing rats with combination of GBN and MRT. (a) The enhancement of gadolinium with proportion to concentration as the contrast. Upper: T₁-weighted, bottom: SPCT. (b) Brain images of 9LGS-bearing rat by T₁-weighted at various time points. Reproduced with permission from Journal of Nanobiotechnology, [173]. Copyright 2020, BioMed Central Ltd. (For interpretation of the references to colour in this figure legend, the reader is referred to the web version of this article.)

increase in ROS and a 7.68-fold increase in OH and O₂ radicals due to X-ray exposure [174]. Le Duc's team of researchers found that the ROS sensor, when coupled with AuNPs, increased ROS generation seven times more when exposed to 6 Gy radiation than when used alone [175]. When exposed to 50 keV X-rays, Gd₂O₃ NPs enhanced ROS production by 1.6 to 1.94. These experiments demonstrate that ROS production radiosensitizes high-Z metal NPs. Scientists made AGuIX NPs for MRI and radiosensitization. These NPs have a Gd₂O₃ core, a polysiloxane shell, and a DTPA chelator. In orthotopic 9LGS gliosarcoma rat models, the kidneys passively sent nanoparticles to the tumor and took them out. ICP-MS measured Gd concentrations in the hemisphere with GBM to be twice as high as in the one without GBM at 20 min post-injection. Within an hour of IV treatment, urine may remove up to 30 % of the Gd component. T1-weighted MRI scans revealed the tumor, demonstrating the effectiveness of the NPs as a T1 contrast agent (Fig. 12, Vb).

The RT and palbociclib RB pathways (cycline-dependent kinase (CDK4/6)) play a key role in controlling the cell cycle. The E2F transcription factor family and the RB tumor suppressor are critical for cell cycle regulation. 86 % of GBM patients exhibit CDK6 amplification and deletions in the CDK inhibitor 2A/B (CDKN2A/B) gene. This is especially true for classical and mesenchymal subtypes. Consistent expression of E2F transcription factors accelerates the cell cycle, duplicates DNA, and advances mitosis [176]. The drug palbociclib (PD0332991; Pfizer) stops the cell cycle and kills RB-competent cells in the lab and in living things [177]. Whittaker et al. found that giving palbociclib in combination with RT improved mice's survival. RT PARP protein inhibitors and poly (ADP ribose) polymerase (PARP) make glioma cells more sensitive to radiation by preventing DNA repair [178]. Studies found that PARP inhibitors (PARPi) reduce colony formation in MGMT-unmethylated GBM patient-generated xenografts. This suggests that PARP inhibition could serve as a novel treatment option for GBM. In glioblastoma CSCs, RT causes an increase in PARP1-mediated DNA damage repair. When PARPi talazoparib (BMN-673; Pfizer) is used for a long time with RT, the G2/M block lasts longer and GSC growth slows down [179].

4.3. Tyrosine kinase receptor inhibitors in combination therapy

GBM frequently exhibits receptor tyrosine kinase (RTK) activation, including EGFR, PDGFR, and MET. The success of TKIs in other malignancies led to the conduct of clinical trials for GBM. TKI outcomes in adult glioblastoma are unfavorable. Clinical study results disappoint. Drawbacks include resistance, extensive inclusion requirements, and poor TKI pharmacokinetics. Using tumor molecular markers as inclusion criteria improves response. RTK expression is not considered in most TKI clinical trials. Most TKI clinical trials involve recurrent GBM, making target expression studies difficult. Recurrent GBM is genetically different from the primary tumor, making surgery less likely. TKI resistance might emerge from alternate receptors, signaling pathways, or cell adaptation to a new environment. TKIs inhibit RTKs, although GBM cells activate several TKs. Stommel and his colleagues found that RTK-inhibitor monotherapy had a weak effect, but using a combination of drugs targeting several active RTKs has improved the results [180]. When combined gefitinib (which blocks EGFR) with cediranib (which blocks VEGF), it improved survival and response rates in patients with recurrent GBM. Additionally, RTK systems can modulate overlapping downstream signaling pathways that contribute to cancer. The malignant development of GBM is associated with EGFR and c-MET. The EGFRVIII mutation makes tumors grow faster and less sensitive to HGF-c-MET pathway inhibitor therapy. On the other side, activating the c-MET pathway decreases tumor growth responses to EGFR inhibitors. Co-targeting c-MET and EGFR pathways has shown significant anti-tumor effects in glioblastoma models. From this perspective, a single RTK inhibitor is not sufficient for the important downstream signaling in complex TME, which suggests that RTK inhibition by a single inhibitor doesn't work properly on these tumors.

4.4. Immunotherapy in combination therapy

Immunosuppression is one of the leading causes of the poor prognosis in GBM. Co-inhibitory receptors on T cells, known as immunological checkpoint molecules, diminish the immune response that T cells initiate [181]. CTLA-4 and PD-1 are two immune checkpoint molecules that, when blocked, cause tumor regression and improve long-term survival [182,183]. Researchers have found that having more myeloid-derived suppressor cells (MDSCs) around the tumor makes the immune system weaker in both animal models and human samples. Blocking the growth of MDSCs with PD-1 or CTLA-4 makes immune-simulated gene therapy work better [184–187]. The discovery of various targets for GBM therapy has resulted from GBM molecular profiling and preclinical studies. Table 6 lists the various interventions used in GBM therapy through clinical trials.

5. Limitations and future prospective

Nanomaterials, as a novel type of material with the potential to pass through biological barriers and precisely target tumors, play a vital role in the administration of various medications, opening up new avenues for the development of sophisticated therapeutics for brain tumor therapy. Depending on their size, NP's EPR effect can allow them to enter tumors rather than non-tumorous tissues. Extended nanomaterial circulation can lead to a maximum half-life in the blood, resulting in extended nanomaterial concentrations. Later, GBM and brain metastases typically exhibit a breakdown of the BBB. Therefore, increased BBB permeability can block the safer EPR effect through nanomaterials. Earlier studies emphasized that encapsulating NPs with polymers like

Table 6

Different intervention or treatment options for the GBM treatment with reference to clinical trials.

S. no.	Intervention or treatment	Clinical trials.gov reference number
1	A randomized, multicenter, adaptive phase 3 study of DSP-7888 dosing emulsion in combination with bevacizumab versus bevacizumab alone in patients with recurrent or progressive glioblastoma following initial therapy (WIZARD 201G)	NCT03149003
2	Phase I/II study to evaluate the safety and clinical efficacy of atezolizumab (aPD-L1) in combination with TMZ and radiation in patients with newly diagnosed GBM	NCT03174197
3	Phase II trial of pulse dosing of Lapatinib in combination with TMZ and regional radiation therapy for up-front treatment of patients with newly-diagnosed GBM	NCT01591577
4	Phase I trial of Pembrolizumab and Vorinostat Combined with TMZ and radiation therapy for newly diagnosed glioblastoma	NCT03426891
5	Phase II trial of the PD-1 antibody Nivolumab in combination with hypo fractionated re-irradiation and Bevacizumab for recurrent MGMT methylated glioblastoma	NCT03743662
6	Phase I study to determine the safety and tolerability of the oral microtubule destabilizer BAL101553 in combination with standard radiation in patients with MGMT promoter unmethylated newly diagnosed glioblastoma	NCT03250299
7	Randomized Phase 3 single blind study of TMZ plus radiation therapy combined with Nivolumab or Placebo in newly diagnosed adult subjects with MGMT-methylated (tumor o6-methylguanine DNA methyltransferase) glioblastoma	NCT02667587
8	Open-Label, multi-center trial of INO-5401 and INO-9012 delivered by electroporation (EP) in combination with REGN2810 in subjects with newly-diagnosed GBM	NCT03491683

PEG prolongs plasma liposome circulation. Since liposomes avoid renal clearance, liposomes under 100 nm have a longer half-life. To achieve an EPR effect, nanomaterials' lipophilicity, size, and ionization potential must be adequately adjustable. In the case of liposomal drug delivery, the lipophilic behavior of liposomes and their enhanced interactions with plasma proteins severely limit the EPR effect, preventing passive diffusion to the blood-brain barrier. Hence, researchers are currently working on active targeted methods to combat glioblastoma and other aggressive tumors. To enhance the effectiveness of active targeting, researchers must thoroughly functionalize nanomaterials using a variety of ligands like peptides, antibodies, and surface proteins [188]. Furthermore, the poor storage stability and insufficient bulk manufacturing of exosomes are hindering their successful drug delivery in glioma. Therefore, we should include prospective clinical studies to demonstrate the beneficial activities of glioma-targeted exosomes in GBM theranostics.

In the case of RT, there are still many obstacles and issues to overcome. Tumor heterogeneity and metabolic abnormalities make radiation challenging to treat malignancies, not just GBM but other cancers. Radiosensitizers improve cell sensitivity to RT by modifying cell components that mitigate radiation damage and without inducing the radiation dosage. Unfortunately, the nonspecific nature of radiosensitizers causes collateral damage to healthy tissue, making it possible to administer only limited doses, which lead to tumor recurrence from surviving populations of radioresistant cells [189]. More importantly, intracellular localization of the NPs influences the radiosensitizing impact. Researchers suggest setting up (i) strategies to target NPs inside cells, preferably at the nucleus or mitochondria, and (ii) using microdosimetry techniques to investigate the various radiosensitizing effects at the micro level. Further research is necessary to determine the characteristics that could enhance the radiosensitizing effect by examining various types of metals, their functions, and their dimensions.

Further research is necessary to clarify the toxicity, stability, safety, and clearance mechanisms of nanotherapeutics for glioma treatment [190]. Most anti-GBM therapies are known to be ineffective due to the complex and unknown properties of the TME. Along with angiogenesis, TME has low oxygen levels, mild acidity, certain redox reactions, high interstitial pressure, and a dense stromal structure. Researchers should carefully consider these features when considering an NPs-based anti-GBM therapeutic approach. Further, researchers should focus more on achieving a uniform distribution of NPs, which in turn depends on the complexity of the TME. Furthermore, it is believed that GBM stem cells, capable of rapid division, tumor formation, cell invasion, and resistance to radiation and chemotherapy, are responsible for the recurrence. Regardless of the therapy type, overcoming certain obstacles can result in persistent GBM treatment. In fact, (i) these issues arise due to the lack of preclinical models that closely mimic human GBM; (ii) it's challenging to do clinical trials on enough patients to get statistically significant clinical data; (iii) clinical trials can only treat GBM patients who are already far along in the disease; and (iv) GBM isn't always found in the early stages. We must overcome these obstacles to find an effective treatment for GBM. The novel and exploratory drugs should be effective in overcoming major hurdles, such as breaking through the BBB, releasing therapeutic payloads that are only successful in tumor cells, and improving patient survival and quality of life. The capacity of chemotherapeutic nanomedicine to handle most of the GBM drug delivery issues is yet unknown, as is the degree of its ability to treat GBM challenges. Therefore, as mentioned earlier, extensive research is necessary to establish nanomedicine strategies as successful treatment approaches. To advance these systems, we must gather more information about toxicological profiles, long-term stability, safety data, and clearance processes for innovative therapeutics. Furthermore, multifunctional NPs will broaden the possibilities for developing improved treatments for brain cancer, allowing for direct evaluation of tumor status in conjunction with therapy that could provide personalized medicine. On the other hand, the translation of these techniques is

purposely sluggish, and only a handful have made it to clinical trials for brain tumor applications. However, since nanotechnology allows for chemical changes and functionalization, researchers may be able to construct comprehensive therapies for brain malignancies that transport drug cargoes and imaging agents.

6. Conclusion

GBM is a highly aggressive glioma that scientists and medical professionals are still struggling to treat. Even with conventional care, patients with GBM have a median survival time of 15 months after the initial diagnosis. Until we achieve breakthroughs that can extend the lives of GBM sufferers, it's critical to keep coming up with new ideas. Extensive research is exploring GBM's aggressive behavior. GBM's flaws are also being discovered. The rapid growth of GBM tissue, as evidenced by necrosis and microvascular proliferation, causes the BBB to become leaky, allowing NPs to pass through. The EPR effect occurs when blocked or damaged lymphatic channels in the brain parenchyma trap NPs in GBM tumor tissue. Nanotechnology's capacity to reach the brain parenchyma is a significant advantage that bodes well for this branch of research in GBM treatment. The benefit of nanotechnology will become more obvious when the selectivity of NPs for GBM tissue improves. The significant characteristics of NPs allow their utility in future GBM research and therapy development. For instance, the strategy of successful surface functionalization of NPs is essential for the targeted administration of chemotherapeutics, particularly for GBM and brain malignancies. Biologically, the surface facilitates contact with the target, and its properties can affect the composition of the protein corona, clearance duration, and system toxicity. Further, the surface composition of NPs is crucial for optimizing the engineering process and ensuring the production of desirable NPs suitable for the development of GBM therapeutics. The significant features for characterizing NPs include size, surface charge, shape, porosity, surface chemistry, crystalline structure, purity, drug loading, and hydrophobicity [191]. Noteworthy, an improper understanding of these characteristics can lead to their non-specific distribution in unintended tissues and premature clearance. Again, the surface interactions of NPs with various biological components determine their behavior in the complex biological environment after administration. Thus, the surface chemistry of NPs greatly influences their solubility, stability, biocompatibility, and pharmacokinetics. In addition, the determination of the ligand density is also a crucial step in defining an NP system, which is essential for improving the design and optimization of NPs with the best ligand density to make them more effective at targeting during formulation.

More importantly, the EPR effect of NPs depends on their size, which permits them to settle down into tumor sites rather than non-tumor sites. Furthermore, prolonged circulation of NPs can result in a maximal half-life in the bloodstream, thereby sustaining their quantities [192]. Consequently, increased permeability of the BBB may hinder the safer EPR effect that NPs can provide. To realize an EPR effect, the lipophilicity, morphology, and ionization potential of NPs must be conveniently tunable [193–195]. On the other hand, actively targeting the BBB and tumor cells with ligands has always been a cornerstone of innovative research; a new alternative has lately emerged. Researchers have discovered that many targeted systems fail due to tumor cells' ability to modify their TME, which can obstruct the immune response or degrade NPs systems. Several critical factors, such as acidic pH, elevated ROS levels, or the presence of solutes and cells obstructing immune recognition, can influence this alteration. Instead of directly attacking the cells, research is focusing on leveraging differences in the TME to activate NPs, regulate drug release, impede tumor spread, and reduce immune system suppression.

A new type of NPs known as biomimetic CMCNPs carries biologically generated CMs and delivers drugs to specific sites, preventing drug accumulation in unwanted areas. Thus, decreasing side effects can improve GBM treatment, especially when CMCNPs carry theranostic

drugs. Researchers are using QGDs and CQDs to tackle GBM due to their fascinating properties. These have photophysical, ultra-nanoscale, electrochemical, fluorescence-tunable, and receptor-based targeting properties. Furthermore, researchers are exploring them as selective nanotheranostics for PDT and PTT applications. Nanotheranostic agents like exosomes are appealing because they are stable in the bloodstream, biocompatible, cause few immune responses, and naturally target cells. Exosomes transport therapeutic proteins, nucleic acids, and lipids to their surfaces, enhancing cell communication. To treat GBM, exosome payloads must vary by origin and biological state. Recent research has focused on GBM theranostic uses of active ligand-functionalized liposomes and LNCs. Overall, this review offers insights into the various advancements and perspectives of nanomaterials in nanotheranostics for the treatment of GBM.

CRedit authorship contribution statement

Roopkumar Sangubotla: Writing – review & editing, Writing – original draft, Validation, Investigation, Data curation, Conceptualization. **Kumar Shiva Gubbiyappa:** Writing – review & editing, Writing – original draft. **Rajakumari Devarapogu:** Writing – review & editing, Writing – original draft. **Jongsung Kim:** Writing – review & editing, Supervision, Resources, Project administration, Funding acquisition.

Declaration of competing interest

The authors declare that they have no known competing financial interests or personal relationships that could have appeared to influence the work reported in this paper.

Acknowledgements

This research was supported by Basic Science Research Program through National Research Foundation of Korea (NRF) funded by the Ministry of Education (2021R1A6A1A03038996) and by the National Research Foundation of Korea (NRF) grant funded by the Korea government (MSIT) (NRF-2022R1A2C1009968).

Data availability

No data was used for the research described in the article.

References

- [1] X. Yu, Y. Jiang, W. Wei, P. Cong, Y. Ding, L. Xiang, K. Wu, *Tumour Biol.* 36 (2015) 967–972.
- [2] O.G. Taylor, J.S. Brzozowski, K.A. Skelding, *Front. Oncol.* 9 (2019) 963.
- [3] Q.T. Ostrom, G. Cioffi, H. Gittleman, N. Patil, K. Waite, C. Kruchko, J. S. Barnholtz-Sloan, *Neuro-Oncology* 21 (2019) v1–v100.
- [4] A.O. Sasmita, Y.P. Wong, A.P. Ling, *Asia Pac. J. Clin. Oncol.* 14 (2018) 40–51.
- [5] C. Chinopoulos, T.N. Seyfried, *ASN Neuro* 18 (2018) 10, <https://doi.org/10.1177/1759091418818261>.
- [6] N.J. Ernest, H. Sontheimer, *Glioma, Brain Res.* 1144 (2007) 231–238.
- [7] B.M. Alexander, T.F. Cloughesy, *J. Clin. Oncol.* 35 (2017) 2402–2409.
- [8] D.N. Louis, A. Perry, G. Reifenberger, A. von Deimling, D. Figarella-Branger, W. K. Cavenee, H. Ohgaki, O.D. Wiestler, P. Kleihues, D.W. Ellison, *Acta Neuropathol.* 131 (2016) 803–820.
- [9] Y.W. Park, P. Vollmuth, M. Foltyn-Dumitru, F. Sahn, S.S. Ahn, J.H. Chang, S. H. Kim, *J. Magn. Reson. Imaging* 58 (2023) 677–689.
- [10] L. Zhang, et al., *Adv. Drug Deliv. Rev.* 190 (2022) 114536.
- [11] K. Nuthalapati, et al., *Small Sci* 4 (2024) 2400191.
- [12] A.D. Bangham, *BioEssays news rev.* *Mol. Cell. Dev. Biol.* 17 (1995) 1081–1088.
- [13] A. Papachristodoulou, R.D. Signorell, B. Werner, D. Brambilla, P. Luciani, M. Cavusoglu, J. Grandjean, M. Silgner, M. Rudin, E. Martin, M. Weller, *J. Control. Release* 295 (2019) 130–139.
- [14] S. Ghanbarzadeh, H. Valizadeh, P. Zakeri-Milani, *Adv Pharm Bull* 3 (2013) 25–29.
- [15] H. Valizadeh, S. Ghanbarzadeh, P. Zakeri-Milani, *Drug Dev. Ind. Pharm.* 2015 (41) (2015) 1558–1565.
- [16] M. Alavi, N. Karimi, M. Safaei, *Adv Pharm Bull* 7 (2017) 3–9.
- [17] A. Akbarzadeh, R. Rezaei-sadabady, S. Davaran, S.W. Joo, N. Zarghami, et al., *Nanoscale Res. Lett.* 8 (2013) 102.
- [18] H. Zhang, *Methods Mol. Biol.* 1522 (2017) 17–22.
- [19] R. Mendez, S. Banerjee, *Methods Mol. Biol.* 1609 (2017) 255–260, <https://doi.org/10.1007/978-1-4939-6996-8-21>.
- [20] R.L. Hamilton Jr., J. Goerke, L.S. Guo, M.C. Williams, R.J. Havel, *J. Lipid Res.* 21 (1980) 981–992.
- [21] A.A. Smirnov, *Biull Eksp Biol Med* 98 (1984) 249–252. Russian. PMID: 6466867.
- [22] D. Patel, K.K. Sawant, *Curr. Drug Deliv.* 6 (2009) 419–424, <https://doi.org/10.2174/156720109789000519>.
- [23] H. Valadi, K. Ekström, A. Bossios, M. Sjöstrand, J.J. Lee, J.O. Lötvall, *Nat. Cell Biol.* 9 (2007) 654–659.
- [24] C. Cossetti, N. Iraci, T.R. Mercer, T. Leonardi, E. Alpi, D. Drago, C. Alfaro-Cervello, H.K. Saini, M.P. Davis, J. Schaeffer, B. Vega, *Mol. Cell* 56 (2014) 193–204.
- [25] L.A. Mulcahy, R.C. Pink, D.R. Carter, *J. Extracell. Vesicles* 3 (2014) 24641.
- [26] G. Pironti, R.T. Strachan, D. Abraham, Yu S. Mon-Wei, M. Chen, W. Chen, K. Hanada, L. Mao, L.J. Watson, H.A. Rockman, *Circulation* 131 (2015) 2120–2130.
- [27] P.R. Lowenstein, R.J. Mandel, W.D. Xiong, K. Kroeger, M.G. Castro, *Curr. Gene Ther.* 7 (2007) 347–360.
- [28] J.S. Zhang, F. Liu, L. Huang, *Adv. Drug Deliv. Rev.* 57 (2005) 689–698.
- [29] T. Ishida, M. Ichihara, X. Wang, K. Yamamoto, J. Kimura, E. Majima, H. Kiwada, *J. Control. Release* 112 (2006) 15–25.
- [30] Z. Shen, et al., *Biomaterials* 235 (2020) 119783.
- [31] P. Chakraborty, et al., *J. Control. Release* 350 (2022) 698–715.
- [32] N. Dhas, et al., *J. Control. Release* 346 (2022) 71–97.
- [33] R.H. Bobo, D.W. Laske, A. Akbasak, P.F. Morrison, R.L. Dedrick, E.H. Oldfield, *Proc. Natl. Acad. Sci.* 91 (1994) 2076–2080.
- [34] S. Kunwar, S. Chang, M. Westphal, M. Vogelbaum, J. Sampson, G. Barnett, M. Shaffrey, Z. Ram, J. Piepmeyer, M. Prados, D. Croteau, *Neuro-Oncol* 12 (2010) 871–881.
- [35] R.C. Anderson, B. Kennedy, C.L. Yanes, J. Garvin, M. Needle, P. Canoll, N. A. Feldstein, J.N. Bruce, *J. Neurosurg. Pediatr.* 11 (2013) 289–295.
- [36] T. Shahar, Z. Ram, A.A. Kanner, *J. Neuro-Oncol.* 107 (2012) 373–378.
- [37] P.Y. Chen, T. Ozawa, D.C. Drummond, A. Kalra, J.B. Fitzgerald, D.B. Kirpotin, K. C. Wei, N. Butowski, M.D. Prados, M.S. Berger, J.R. Forsayeth, *Neuro-Oncol* 15 (2013) 189–197.
- [38] R.R. Lonser, S. Walbridge, K. Garmestani, J.A. Butman, H.A. Walters, A. O. Vortmeyer, P.F. Morrison, M.W. Brechbiel, E.H. Oldfield, *Successful and safe perfusion of the primate brainstem: in vivo magnetic resonance imaging of macromolecular distribution during infusion*, *J. Neurosurg.* 97 (2002) 905–913.
- [39] X. Yang, R. Saito, T. Nakamura, R. Zhang, Y. Sonoda, T. Kumabe, J. Forsayeth, K. Bankiewicz, T. Tominaga, *Drug Deliv.* 23 (2016) 771–776.
- [40] A.A. Linninger, M.R. Somayaji, M. Mekarski, L. Zhang, *J. Theor. Biol.* 250 (2008) 125–138.
- [41] J.H. Sampson, M. Brady, R. Raghavan, A.I. Mehta, A.H. Friedman, D.A. Reardon, N.A. Petry, D.P. Barboriak, T.Z. Wong, M.R. Zalutsky, D. Lally-Goss, *Neurosurgery* 69 (2011) 668–676.
- [42] J.M. Stukel, M.R. Caplan, *Expert Opin. Drug Deliv.* 6 (2009) 705–718.
- [43] E. White, A. Bienemann, J. Pugh, E. Castrique, M. Wyatt, H. Taylor, A. Cox, C. Mcleod, S. Gill, *J. Neuro-Oncol.* 108 (2012) 77–88.
- [44] J.N. Bruce, R.L. Fine, P. Canoll, J. Yun, B.C. Kennedy, S.S. Rosenfeld, S.A. Sands, K. Surapaneni, R. Lai, C.L. Yanes, E. Bagiella, *Neurosurgery* 69 (2011) 1272–1280.
- [45] M.S. Fianadca, V. Varenika, J. Eberling, T. McKnight, J. Bringas, P. Pivrotto, J. Beyer, P. Hadaczek, W. Bowers, J. Park, H. Federoff, *Neuroimage* 47 (2009) T27–T35.
- [46] K. Bankiewicz, K.H. Rosenbluth, A.J. Martin, S. Mittermeyer, J. Eschermann, P. J. Dickinson, K.S. Bankiewicz, *PLoS One* 8 (2013) e56397.
- [47] L. Bobyk, M. Edouard, P. Deman, M. Vautrin, K. Pernet-Gallay, J. Delaroche, J. F. Adam, F. Estève, J.L. Ravanat, H. Elleaume, *Nanomedicine* 9 (2013) 1089–1097.
- [48] S. Her, D.A. Jaffray, C. Allen, *Adv. Drug Deliv. Rev.* 109 (2017) 84–101.
- [49] J. Liu, Q. Peng, *Acta Biomater.* 55 (2017) 13–27.
- [50] U.K. Sukumar, R.J.C. Bose, M. Malhotra, H.A. Babikir, R. Afjei, E. Robinson, Y. Zeng, E. Chang, F. Habte, R. Sinclair, et al., *Biomaterials* 218 (2019) 119342.
- [51] T. Coccini, S. Grandi, D. Lonati, C. Locatelli, U. De Simone, *Neurotoxicol* 48 (2015) 77–89.
- [52] J. Bourquin, A. Milosevic, D. Hauser, R. Lehner, F. Blank, A. Petri-Fink, *Adv. Mater.* 30 (2018) e1704307.
- [53] E. Luque-Michel, L. Lemaire, M.J. Blanco-Prieto, *Drug Deliv. Transl. Res.* 11 (2021) 515–523.
- [54] M.-H. Chan, et al., *ACS Appl. Mater. Interfaces* 13 (2021) 26759–26769.
- [55] Z. Lv, L. Jin, Y. Cao, et al., *Light Sci Appl.* 11 (2022) 116.
- [56] F. Zhang, X. Huang, L. Zhu, N. Guo, G. Niu, M. Swierczewska, S. Lee, H. Xu, A. Y. Wang, K.A. Mohamedali, M.G. Rosenblum, *Biomaterials* 33 (2012) 5414–5422.
- [57] J. Kolosnjaj-Tabi, R. Di Corato, L. Lartigue, I. Marangon, P. Guardia, A.K. Silva, N. Luciani, O. Clement, P. Flaud, J.V. Singh, P. Decuzzi, *ACS Nano* 8 (2014) 4268–4283.
- [58] A.C. Silva, T.R. Oliveira, J.B. Mamani, S.M. Malheiros, L. Malavolta, L.F. Pavon, T.T. Sibov, E. Amaro Jr., A. Tannús, E.L. Vidoto, M.J. Martins, *Int. J. Nanomedicine* 6 (2011) 591.
- [59] K. Mahmoudi, A. Bouras, D. Bozec, R. Ivkov, C. Hadjipanayis, *Int. J. Hyperth.* 34 (2018) 1316–1328.
- [60] I. Tsiapa, E.K. Efthimiadou, E. Fragogeorgi, G. Loudos, A.D. Varvarigou, P. Bouziotis, G.C. Kordas, D. Mihailidis, G.C. Nikiforidis, S. Xanthopoulos, D. Psimadas, *J. Colloid Interface Sci.* 433 (2014) 163–175.

- [61] B.A. Lakshmi, Y.J. Kim, *Int. J. Mol. Sci.* 23 (2022) 1641.
- [62] H. Chen, L. Shao, Q. Li, J. Wang, *Chem. Soc. Rev.* 42 (2013) 2679–2724.
- [63] J. Beik, Z. Abed, F.S. Ghoreishi, S. Hosseini-Nami, S. Mehrzadi, A. Shakeri-Zadeh, S.K. Kamrava, *J. Control. Release* 235 (2016) 205–221.
- [64] T.F. Cabada, C.S. de Pablo, A.M. Serrano, Guerrero F. del Pozo, J.J. Olmedo, M. R. Gomez, *Int. J. Nanomedicine* 7 (2012) 1511.
- [65] J. Choi, J. Yang, J. Park, E. Kim, J.S. Suh, Y.M. Huh, S. Haam, *Adv. Funct. Mater.* 21 (2011) 1082–1088.
- [66] A. Agarwal, M.A. Mackey, M.A. El-Sayed, R.V. Bellamkonda, *ACS Nano* 5 (2011) 4919–4926.
- [67] M. Oli, *Medicine* 3 (2010) 18.
- [68] R. Tenchov, R. Bird, A.E. Curtze, Q. Zhou, *ACS Nano* 15 (2021) 16982–17015.
- [69] M. Alibolandi, F. Charbgoon, S.M. Taghdisi, K. Abnous, M. Ramezani, *Academic Press* 1 (2018) 75–110.
- [70] S. Gao, H. Tian, Z. Xing, D. Zhang, Y. Guo, Z. Guo, X. Zhu, X. Chen, *J. Control. Release* 243 (2016) 357–369.
- [71] M. Sánchez-Navarro, E. Giral, M. Teixidó, *Curr. Opin. Chem. Biol.* 38 (2017) 134–140.
- [72] M. Kristensen, B. Brodin, *J. Pharm. Sci.* 106 (2017) 2326–2334.
- [73] E.A. Disalvo, A.M. Bouchet, *Colloids Surf. A Physicochem. Eng. Asp.* 440 (2014) 170–174.
- [74] A.S. Timin, M.M. Litvak, D.A. Gorin, E.N. Atochina-Vasserman, D.N. Atochin, G. B. Sukhorukov, *Adv. Healthc. Mater.* 7 (2018) 1700818.
- [75] M. Charabati, J.M. Rabanel, C. Ramassamy, A. Prat, *Trends Pharmacol. Sci.* 41 (2020) 42–54.
- [76] X. Liu, X. Yi, J. Gu, Z. Ji, M. Zhu, M. Shen, Y. Ren, L. Guo, T. Liu, N. Ding, K. Yang, *Nano Today* 53 (2023) 102037.
- [77] J. Kuang, Z.Y. Rao, D.W. Zheng, D. Kuang, Q.X. Huang, T. Pan, H. Li, X. Zeng, X. Z. Zhang, *ACS Nano* 17 (2023) 13333–13347.
- [78] D. Mendanha, J. Vieira de Castro, M.R. Casanova, S. Gimondi, H. Ferreira, N. M. Neves, *Nanomedicine Nanotechnology, Biol. Med.* 49 (2023) 102663.
- [79] V.P. Gibson, *Biomaterials* 302 (2023) 122341.
- [80] W. Wu, J.L. Klockow, M. Zhang, F. Lafortune, E. Chang, L. Jin, Y. Wu, H. E. Daldrop-Link, *Pharmacol. Res.* 171 (2021) 105780.
- [81] C. Zhao, et al., *Biomed. Pharmacother.* 171 (2024) 116113.
- [82] P. Kadiyala, D. Li, F.M. Nuñez, D. Altschuler, R. Doherty, R. Kuai, M. Yu, N. Kamran, M. Edwards, J.J. Moon, P.R. Lowenstein, *ACS Nano* 13 (2019) 1365–1384.
- [83] A. Grillone, M. Battaglini, S. Moscato, L. Mattii, Fernández C. de Julián, A. Scarpellini, M. Giorgi, E. Sinibaldi, G. Ciofani, *Nanomed* 8 (2019) 727–752.
- [84] C. Tapeinos, A. Marino, M. Battaglini, S. Migliorin, R. Brescia, A. Scarpellini, C. D. Fernández, M. Prato, F. Drago, G. Ciofani, *Nanoscale* 11 (2019) 72–88.
- [85] D.K. Flak, V. Adamski, G. Nowaczyk, K. Szutkowski, M. Synowitz, S. Jurga, *J. Held-Feindt, Int. J. Nanomedicine* 15 (2020) 7415.
- [86] T. Ahmed, F.C. Liu, C. He, A.Z. Abbasi, P. Cai, A.M. Rauth, J.T. Henderson, X. Y. Wu, *Pharm. Res.* 38 (2021) 1897–1914.
- [87] E. Gajda, M. Godlewska, Z. Mariak, E. Nazaruk, D. Gawel, *Int. J. Mol. Sci.* 21 (2020) 5039.
- [88] S.L. Hayward, C.L. Wilson, S. Kidambi, *Oncotarget* 7 (2016) 34158.
- [89] L. Battaglia, E. Ugazio, *J. Nanomater.* 2019 (2019).
- [90] N. Anton, J.P. Benoit, P. Saulnier, *J. Control. Release* 128 (2008) 185–199.
- [91] C.R. Mouzouvi, A. Umerska, A.K. Bigot, P. Saulnier, *PLoS One* 12 (2017) e0179211.
- [92] K. Coradini, R.B. Friedrich, F.N. Fonseca, M.S. Vencato, D.F. Andrade, C. M. Oliveira, A.P. Battistel, S.S. Guterres, M.I. da Rocha, A.R. Pohlmann, R. C. Beck, *Eur. J. Pharm. Sci.* 78 (2015) 163–170.
- [93] N.T. Huynh, C. Passirani, P. Saulnier, J.P. Benoit, *Int. J. Pharm.* 379 (2009) 201–209.
- [94] Z. Niu, I. Conejos-Sánchez, B.T. Griffin, C.M. O’Driscoll, M.J. Alonso, *Adv. Drug Deliv. Rev.* 106 (2016) 337–354.
- [95] A.A. Ramadan, *Université d’Angers*, 2010.
- [96] C. Dulieu, D. Bazile, *Pharm. Res.* 22 (2005) 285–292.
- [97] B. Heurtault, P. Saulnier, B. Pech, J.E. Proust, J.P. Benoit, *Int. J. Pharm.* 242 (2002) 167–170.
- [98] C.H. Kim, S.G. Lee, M.J. Kang, S. Lee, Y.W. Choi, *J. Pharm. Investig.* 47 (2017) 203–227.
- [99] D. Hoarau, P. Delmas, S. David, E. Roux, J.C. Leroux, *Pharm. Res.* 21 (2004) 1783–1789.
- [100] N. Dabholkar, T. Waghule, V.K. Rapalli, S. Gorantla, A. Alexander, R.N. Saha, G. Singhvi, *J. Mol. Liq.* 339 (2021) 117145.
- [101] J. Aparicio-Blanco, V. Sebastián, J.P. Benoit, A.I. Torres-Suárez, *Eur. J. Biopharm* 134 (2019) 126–137.
- [102] A. Clavreul, E. Roger, M. Pourbaghi-Masouleh, L. Lemaire, C. Tétaud, P. Menei, *Drug Deliv.* 25 (2018) 1756–1765.
- [103] C. Bastiancich, E. Bozzato, U. Luyten, F. Danhier, G. Bastiat, V. Préat, *Int. J. Pharm.* 559 (2019) 220–227.
- [104] N.R. Pereira, R.A. Loiola, S.F. Rodrigues, C.P. de Oliveira, S.L. Büttgenbender, S. S. Guterres, A.R. Pohlmann, S.H. Farsky, *Int. J. Nanomedicine* 13 (2018) 4563.
- [105] F. Najlaoui, P. Pigeon, S. Aroui, M. Pezet, L. Sancey, N. Marrakchi, A. Rhouma, G. Jaouen, M. De Waard, B. Busser, S. Gibaud, *J. Pharm. Pharmacol.* 70 (2018) 1474–1484.
- [106] F. Danhier, K. Messaoudi, L. Lemaire, J.P. Benoit, F. Lagarce, *Int. J. Pharm.* 481 (2015) 154–161.
- [107] M. Roger, A. Clavreul, N.T. Huynh, C. Passirani, P. Schiller, A. Vessières, C. Montero-Menei, P. Menei, *Int. J. Pharm.* 423 (2012) 63–68.
- [108] J. Mattiazzi, M.H. Sari, R. Lautenchleger, M. Dal Prá, E. Braganhol, L. Cruz, *AAPS. Pharm. Sci. Tech* 20 (2019) 49.
- [109] G. Raposo, W. Stoorvogel, *J. Cell Biol.* 200 (2013) 373–383.
- [110] J.E. Pullan, M.I. Confeld, J.K. Osborn, J. Kim, K. Sarkar, S. Mallik, *Mol. Pharm.* 16 (2019) 1789–1798.
- [111] D. Yang, et al., *Theranostics* 10 (2020) 3684–3707.
- [112] W. Sun, J.D. Luo, H. Jiang, D.D. Duan, *Acta Pharmacol. Sin.* 39 (2018) 534–541.
- [113] N.L. Syn, L. Wang, E.K. Chow, C.T. Lim, B.C. Goh, *Trends Biotechnol.* 35 (2017) 665–676.
- [114] C. Théry, *Annu. Rev. Cell Dev. Biol.* 30 (2014) 255–289.
- [115] C. Théry, L. Zitvogel, S. Amigorena, *Nat. Rev. Immunol.* 2 (2002) 569–579.
- [116] M. Simons, G. Raposo, *Curr. Opin. Cell Biol.* 21 (2009) 575–581.
- [117] X. Zhuang, X. Xiang, W. Grizzle, D. Sun, S. Zhang, R.C. Axtell, S. Ju, J. Mu, L. Zhang, L. Steinman, D. Miller, *Mol. Ther.* 19 (2011) 1769–1779.
- [118] T. Yang, P. Martin, B. Fogarty, A. Brown, K. Schurman, R. Phipps, V.P. Yin, P. Lockman, S. Bai, *Pharm. Res.* 32 (2015) 2003–2014.
- [119] T.N. Lamichhane, R.S. Raiker, S.M. Jay, *Mol. Pharm.* 12 (2015) 3650–3657.
- [120] M. Hadla, S. Palazzolo, G. Corona, I. Caligiuri, V. Canzonieri, G. Toffoli, *F. Rizzolio, Nanomedicine* 11 (2016) 2431–2441.
- [121] M.S. Kim, M.J. Haney, Y. Zhao, V. Mahajan, I. Deygen, N.L. Klyachko, E. Inskoe, A. Piroyan, M. Sokolsky, O. Okolie, S.D. Hingtgen, *Nanomed.: Nanotechnol. Biol. Med.* 12 (2016) 655–664.
- [122] T.N. Lamichhane, A. Jeyaram, D.B. Patel, B. Parajuli, N.K. Livingston, N. Arumugasamy, J.S. Schardt, S.M. Jay, *Cell. Mol. Bieng.* 9 (2016) 315–324.
- [123] M.J. Haney, N.L. Klyachko, Y. Zhao, R. Gupta, E.G. Plotnikova, Z. He, T. Patel, A. Piroyan, M. Sokolsky, A.V. Kabanov, E.V. Batrakova, *J. Control. Release* 207 (2015) 18–30.
- [124] Y.T. Sato, K. Umezaki, S. Sawada, S.A. Mukai, Y. Sasaki, N. Harada, H. Shiku, K. Akiyoshi, *Sci. Rep.* 6 (2016) 21933.
- [125] S.S. Yerneni, E. Lathwal, P. Shrestha, H. Shirwan, K. Matyjaszewski, L. Weiss, E. S. Yolcu, P.G. Campbell, S.R. Das, *ACS Nano* 13 (2019) 10555–10565.
- [126] C. Martinelli, F. Gabriele, E. Dini, F. Carriero, G. Bresciani, B. Slivinski, M. Dei Giudici, L. Zanoletti, F. Manai, M. Paolillo, S. Schinelli, *Cells* 9 (2020) 1626.
- [127] A.N. Kenari, L. Cheng, A.F. Hill, *Methods* 177 (2020) 103–113.
- [128] S. Kalimuthu, P. Gangadaran, R.L. Rajendran, L. Zhu, J.M. Oh, H.W. Lee, A. Gopal, S.H. Baek, S.Y. Jeong, S.W. Lee, J. Lee, *Front. Pharmacol.* 9 (2018) 1116.
- [129] A. Nasiri Kenari, K. Kastaniegaard, D.W. Greening, M. Shambrook, A. Stensballe, L. Cheng, A.F. Hill, *Proteomics* 19 (2019) 1800161.
- [130] X. Fang, et al., *J. Am. Chem. Soc.* 146 (2024) 15251–15263.
- [131] M.L. Hill, et al., *ACS Appl. Mater. Interfaces* 16 (2024) 20286–20301.
- [132] C.L. Davidson, R. Vengoji, M. Jain, S.K. Batra, N. Shonka, *Cancer Lett.* 582 (2024) 216592.
- [133] J. Zeng, A.P. See, J. Phallen, C.M. Jackson, Z. Belcaid, J. Ruzevick, N. Durham, C. Meyer, T.J. Harris, E. Albesiano, G. Pradilla, *Int. J. Radiat. Oncol. Biol. Phys.* 86 (2013) 343–349.
- [134] L. Manterola, et al., *Neuro-Oncology* 16 (2014) 520–527.
- [135] H.G. Xu, G.J. Wang, H.F. Liu, Y.H. Zhang, *Springer Singapore* 503 (2019) 381–391.
- [136] X. Zhuang, X. Xiang, W. Grizzle, D. Sun, S. Zhang, R.C. Axtell, S. Ju, J. Mu, L. Zhang, L. Steinman, D. Miller, H.G. Zhang, *Mol. Ther.* 19 (2011) 1769–1779.
- [137] M. Katakowski, B. Buller, X. Zheng, Y. Lu, T. Rogers, O. Osobamiro, W. Shu, F. Jiang, M. Chopp, *Cancer Lett.* 335 (2013) 201–204.
- [138] M.F. Mcdonald, et al., *Neuro-Oncology* 26 (2024) 236–250.
- [139] L. Zhu, J.M. Oh, P. Gangadaran, S. Kalimuthu, S.H. Baek, S.Y. Jeong, S.W. Lee, J. Lee, B.C. Ahn, *Front. Immunol.* (2018) 9.
- [140] Z. Zhang, J. Yin, C. Lu, Y. Wei, A. Zeng, Y. You, *J. Exp. Clin. Cancer Res.* 38 (2019) 1–6.
- [141] C. Zhang, J. Song, L. Lou, X. Qi, L. Zhao, B. Fan, G. Sun, Z. Lv, Z. Fan, B. Jiao, *J. Yang, Bioeng. transl. med* 6 (2021) e10203.
- [142] H. Monfared, Y. Jahangard, M. Nikkhal, J. Mirnajafi-Zadeh, S.J. Mowla, *Front. Oncol.* 9 (2019) 782.
- [143] E. Valipour, F.E. Ranjbar, M. Mousavi, J. Ai, Z.V. Malekshahi, N. Mokberian, Z. Taghdiri-Nooshabadi, M. Khanmohammadi, V.T. Nooshabadi, *Microvasc. Res.* 21 (2022) 104385.
- [144] H. Lee, K. Bae, A.R. Baek, E.B. Kwon, Y.H. Kim, S.W. Nam, G.H. Lee, Y. Chang, *Pharmaceutics* 14 (2022) 1002.
- [145] R. Kretowski, M. Kusaczuk, M. Naumowicz, J. Kotynska, B. Szyńska, M. Cechowska-Pasko, *Nanomaterials* 7 (2017) 230.
- [146] I.Y. Kim, E. Joachim, H. Choi, K. Kim, *Nanomedicine* 11 (2015) 1407–1416.
- [147] M. Yazdimaghani, P.J. Moos, M.A. Dobrovolkskaia, H. Ghandehari, *Nanomedicine* 16 (2019) 106–125.
- [148] X. Dong, Z. Wu, X. Li, L. Xiao, M. Yang, Y. Li, J. Duan, Z. Sun, *Int. J. Nanomedicine* 15 (2020) 9089–9113.
- [149] M. Luo, G. Lewik, J.C. Ratcliffe, C.H.J. Choi, E. Makila, W.Y. Tong, N.H. Voelcker, *ACS Appl. Mater. Interfaces* 11 (2019) 33637–33649.
- [150] S. Sheykhzadeh, M. Luo, B. Peng, J. White, Y. Abdalla, T. Tang, E. Mäkilä, N. H. Voelcker, W.Y. Tong, *Sci. Rep.* 10 (2020) 2320.
- [151] O. Turan, P.A. Bielecki, V. Perera, M. Lorkowski, G. Covarrubias, K. Tong, A. Yun, G. Loutrianakis, S. Raghunathan, Y. Park, et al., *Adv. Ther.* 2 (2019) 1900118.
- [152] R. Sun, M. Liu, Z. Xu, B. Song, Y. He, H. Wang, *Nano Res.* 15 (2022) 7392–7401.
- [153] N. Denora, A. Trapani, V. Laquintana, A. Lopedota, G. Trapani, *Curr. Top. Med. Chem.* 9 (2009) 182–196.
- [154] H. Lopez-Bertoni, K.L. Kozielski, Y. Rui, B. Lal, H. Vaughan, D.R. Wilson, N. Mihelson, C.G. Eberhart, J. Laterra, J.J. Green, *Nano Lett.* 18 (2018) 4086–4094.

- [155] Y. Liu, M. Zheng, M. Jiao, C. Yan, S. Xu, Q. Du, M. Morsch, J. Yin, B. Shi, *Biomaterials* 276 (2021) 121036.
- [156] S. Li, W. Su, H. Wu, T. Yuan, C. Yuan, J. Liu, G. Deng, X. Gao, Z. Chen, Y. Bao, *Nat. Biomed. Eng.* 4 (2020) 704–716.
- [157] Z. Li, et al., *Small* 18 (2021) 2105160.
- [158] S.D. Hettiarachchi, R.M. Graham, K.J. Mintz, Y. Zhou, S. Vanni, Z. Penga, R. M. Leblanc, *Nanoscale* 11 (2019) 6192–6205.
- [159] J. Li, et al., *Adv. Funct. Mater.* 31 (2021) 2100969.
- [160] G. Perini, et al., *Int. J. Mol. Sci.* 21 (2020) 6301.
- [161] Y. Xiao, H. Hong, V.Z. Matson, A. Javadi, W. Xu, Y. Yang, Y. Zhang, J.W. Engle, R. J. Nickles, W. Cai, D.A. Steeber, *Theranostics* 2 (2012) 757.
- [162] N.K. Mehra, N.K. Jain, *Mol. Pharm.* 12 (2015) 630–643.
- [163] C.H. Wang, S.H. Chiou, C.P. Chou, Y.C. Chen, Y.J. Huang, C.A. Peng, *Nanomedicine* 7 (2011) 69–79.
- [164] L. Liu, X. Bai, M.V. Martikainen, A. Kärilund, M. Roponen, W. Xu, G. Hu, E. Tasciotti, V.P. Lehto, *Nat. Commun.* 12 (2021) 1–12.
- [165] L. Wu, Q. Li, J. Deng, J. Shen, W. Xu, W. Yang, B. Chen, Y. Du, W. Zhang, F. Ge, S. Lei, K. Li, Z. Wang, *Int. J. Nanomedicine* 16 (2021) 8433–8446.
- [166] R. Ke, X. Zhen, H.S. Wang, L. Li, H. Wang, S. Wang, X. Xie, *J. Colloid Interface Sci.* 609 (2022) 307–319.
- [167] F. Hanif, K. Muzaffar, K. Perveen, S.M. Malhi, S.U. Simjee, *Asian Pac. J. Cancer Prev.* 18 (2017) 3–9.
- [168] A. Shergalis, A. Bankhead III, U. Luesakul, N. Muangsins, N. Neamati, *Pharmacol. Rev.* 70 (2018) 412–445.
- [169] A.L. Iorio, M. da Ros, L. Genitori, M. Lucchesi, F. Colelli, G. Signorino, F. Cardile, G. Laffi, M. de Martino, C. Pisano, I. Sardi, *Oncotarget* 8 (2017) 89595.
- [170] S.S. Kim, A. Rait, E. Kim, K.F. Pirolo, E.H. Chang, *Nanomedicine* 11 (2015) 301–311.
- [171] F.C. Lam, S.W. Morton, J. Wyckoff, T.L. Vu Han, M.K. Hwang, A. Maffa, E. Balkanska-Sinclair, M.B. Yaffe, S.R. Floyd, P.T. Hammond, *Nat. Commun.* 9 (2018) 1991.
- [172] F. Lan, Q. Pan, H. Yu, X. Yue, *J. Neurochem.* 134 (2015) 811–818.
- [173] J. Choi, G. Kim, S. Bin Cho, H.J. Im, *J. Nanobiotechnology.* 18 (2020) 1–23.
- [174] M. Misawa, J. Takahashi, *Nanomedicine nanotechnology, Biol. Med.* 7 (2011) 604–614.
- [175] G. Le Duc, et al., *ACS Nano* 5 (2011) 9566–9574.
- [176] E.S. Knudsen, J.Y. Wang, Targeting the RB-pathway in cancer therapy, *Clin. Cancer Res.* 16 (2010) 1094–1099.
- [177] K.E. Parrish, J. Pokorny, R.K. Mittapalli, K. Bakken, J.N. Sarkaria, W.F. Elmquist, *J. Pharmacol. Exp. Ther.* 355 (2015) 264–271.
- [178] S. Whittaker, D. Madani, S. Joshi, S.A. Chung, T. Johns, B. Day, M. Khasraw, K. L. McDonald, *Cell Death Dis.* 3 (2017) 1–6.
- [179] P. Lesueur, F. Chevalier, E.A. El-Habr, M.P. Junier, H. Chneiweiss, L. Castéra, E. Müller, D. Stefan, Y. Saintigny, *Sci. Rep.* 8 (2018) 1–2.
- [180] J.M. Stommel, A.C. Kimmelman, H. Ying, R. Nabioullin, A.H. Ponugoti, R. Wiedemeyer, A.H. Stegh, J.E. Bradner, K.L. Ligon, C. Brennan, L. Chin, *Science* 318 (2007) 287–290.
- [181] J. Park, M. Kwon, K.H. Kim, J.H. Chang, E.C. Shin, *The. J. Immunol* (2017) 198.
- [182] P.E. Fecci, H. Ochiai, D.A. Mitchell, P.M. Grossi, A.E. Sweeney, G.E. Archer, T. Cummings, J.P. Allison, D.D. Bigner, J.H. Sampson, *Clin. Cancer Res.* 13 (2007) 2158–2167.
- [183] D.M. Pardoll, *Nat. Rev. Cancer* 12 (2012) 252–264.
- [184] J. Zeng, A.P. See, J. Phallen, C.M. Jackson, Z. Belcaid, J. Ruzevick, N. Durham, C. Meyer, T.J. Harris, E. Albesiano, G. Pradilla, *Int. J. Radiat. Oncol. Biol. Phys.* 86 (2013) 343–349.
- [185] B. Raychaudhuri, P. Rayman, J. Ireland, J. Ko, B. Rini, E.C. Borden, J. Garcia, M. A. Vogelbaum, J. Finke, *Neuro-Oncol* 13 (2011) 591–599.
- [186] B. Raychaudhuri, P. Rayman, P. Huang, M. Grabowski, D. Hambardzumyan, J. H. Finke, M.A. Vogelbaum, *J. Neuro-Oncol.* 122 (2015) 293–301.
- [187] N. Kamran, P. Kadiyala, M. Saxena, M. Candolfi, Y. Li, M.A. Moreno-Ayala, N. Raja, D. Shah, P.R. Lowenstein, M.G. Castro, *Mol. Therapy* 25 (2017) 232–248.
- [188] K. Aloss, P. Hamar, *Biochim. Biophys. Acta-Rev. Cancer* 1879 (2024) 189109.
- [189] R. Li, H. Wang, Q. Liang, L. Chen, J. Ren, *Biomater. Sci.* 10 (2022) 892–908.
- [190] Q. Chen, J. Wu, Q. Ye, F. Ma, Q. Zhu, Y. Wu, C. Shan, X. Xie, D. Li, X. Zhan, C. Li, *mBio* 9 (2018) e01683-18.
- [191] F. Rodà, R. Caraffi, S. Picciolini, G. Tosi, M.A. Vandelli, B. Ruozi, M. Bedoni, I. Ottonelli, J.T. Duskey, *Int. J. Mol. Sci.* 24 (2023) 2496.
- [192] X. Kan, J. Ma, J. Ma, D. Li, F. Li, Y. Cao, C. Huang, Y. Li, P. Liu, *Colloids Surf. B: Biointerfaces* 245 (2025) 114328.
- [193] T.F. Docrat, A.O.E. Eltahir, A.A. Hussein, J.L. Marnewick, *Drug Discov. Today* 29 (2024) 104219.
- [194] J. Guo, Z. Zhao, Z.F. Shang, Z. Tang, H. Zhu, K. Zhang, *Exploration* 3 (2023) 20220119.
- [195] Y. Guo, Z. Wang, X. Shi, M. Shen, Engineered cancer cell membranes: an emerging agent for efficient cancer theranostics, *Exploration* 2 (2022) 20210171.